Tracking the Feature Dynamics in LLM Training: A Mechanistic Study

Yang Xu [1] **Yi Wang** [1] **Hao Wang** [1]

Abstract

Understanding training dynamics and feature evolution is crucial for the mechanistic interpretability of large language models (LLMs). Although sparse autoencoders (SAEs) have been used to identify features within LLMs, a clear picture of how these features evolve during training remains elusive. In this study, we: (1) introduce SAE-Track, a novel method to efficiently obtain a continual series of SAEs; (2) mechanistically investigate feature formation and develop a progress measure for it ; and (3) analyze and visualize feature drift during training. Our work provides new insights into the dynamics of features in LLMs, enhancing our understanding of training mechanisms and feature evolution.

1. Introduction

As LLMs increase in size and complexity, understanding their internal mechanisms has become a critical challenge. One notable phenomenon is *polysemanticity*, where individual neurons respond to mixtures of seemingly unrelated inputs, which complicates interpretability. This phenomenon is hypothesized to arise from the superposition of features, as demonstrated in (Elhage et al., 2022), which is based on the linear representation hypothesis (Park et al., 2023). A prominent approach to addressing *polysemanticity* in LLMs involves using SAEs (Bricken et al., 2023; Templeton et al., 2024). SAEs provide a dictionary learning framework to disentangle overlapping features in activation spaces, enabling the identification of more interpretable features. Studies have shown that SAEs can reveal interpretable representations (Bricken et al., 2023; Cunningham et al., 2023), scale to larger models such as Claude 3 Sonnet (Templeton et al., 2024), uncover structures in representations (Li et al., 2024), and analyze non-linear representations (Engels et al., 2024).

Recent work has compared features across different settings—such as different layers (Jack Lindsey et al., 2024; Balagansky et al., 2024), between base and fine-tuned models (Jack Lindsey et al., 2024; Connor Kissane et al., 2024; Taras Kutsyk, 2024), and across different model scales (Lan et al., 2024). However, training dynamics remain underexplored, despite their importance in understanding the mechanisms underpinning LLM behavior.

There are some mechanistic interpretability studies related to training dynamics, but they mostly focus on specific abilities: (Olsson et al., 2022) linked the emergence of in-context learning ability to the development of induction heads; (Nanda et al., 2023) analyzed grokking and its relationship to generalization; (Qian et al., 2024) studied the trustworthiness development of LLMs during pre-training; and (Li et al., 2023) explored the formation of topic structures throughout training. However, using SAEs to study training dynamics offers a new perspective on the evolution of feature semantics and geometry throughout the entire training process.

In this paper, we address these gaps by conducting a comprehensive mechanistic analysis of feature evolution during the training of LLMs. Specifically, we propose SAE-Track and use it to study how features develop and stabilize in semantic meaning, and how they undergo directional changes. By doing so, we uncover novel insights into the evolution of feature semantics and geometry during training.

Our contributions are summarized as follows:

- **SAE-Track**: We introduce a novel method for efficiently tracking feature evolution in LLMs through a continual SAE series across training checkpoints. SAE-Track enables detailed and reliable analysis of feature dynamics (Sec. 2).
- **Feature Semantic Evolution Phases and Patterns**: Using SAE-Track, we identify three distinct phases of feature semantic evolution—*Initialization & Warmup*, *Emergent*, and *Convergent*—as well as three primary transformation patterns: *Maintaining*, *Shifting*, and *Grouping* (Sec. 3).
- **Investigation of Feature Formation**: We define the concept of feature regions and study feature formation based on this foundation. Furthermore, we introduce the Progress Measure to quantify the evolution of features (Sec. 4).

[1]Department of Computer Science, Rutgers University, New Jersey, USA. Correspondence to: Hao Wang <hw488@cs.rutgers.edu>.

Preprint.

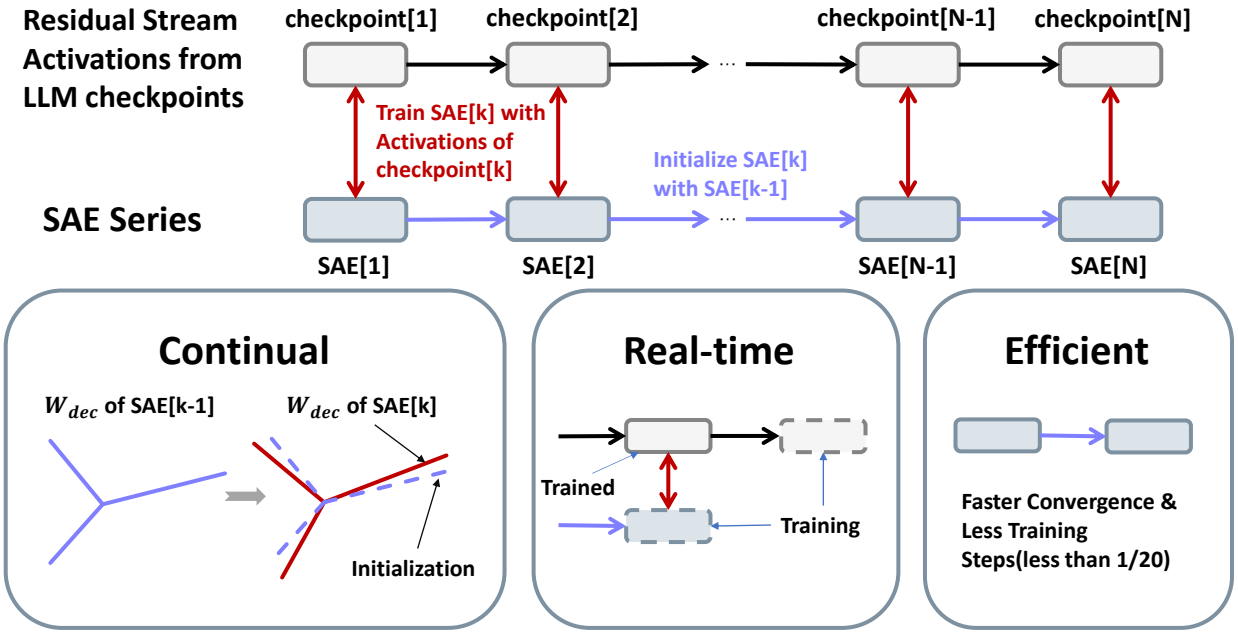

Figure 1. **Illustration of the SAE-Track Framework.** Sparse Autoencoders (SAEs) are trained on residual stream activations from sequential training checkpoints (checkpoint[k]). Each SAE[k] is initialized using parameters from the previously trained SAE[$k-1$]. This approach ensures the **continuity of the SAE** across LLM checkpoints, **Real-Time Training** aligned with the availability of checkpoints, and **Efficient Convergence**, significantly reducing training steps.

- **Analysis of Feature Drift**: We analyze feature drift, focusing on the directional evolution and trajectories of features. For a specific feature, its direction is the normalized decoder vector, while its trajectory is the decoder vector across training checkpoints, both of which capture the directional evolution of features. Our study reveals that feature initially exhibit significant drift, continue to drift even after features are considered "formed," and ultimately stabilize to their final state (Sec. 5).
- **Experiments on Models of Different Scales**: We validate our findings using open-source LLM checkpoints, including Pythia (Biderman et al., 2023) and Stanford CRFM Mistral GPT-2 (Karamcheti et al., 2021), with models of varying scales (Pythia: 160M, 410M, 1.4B; Stanford CRFM GPT-2: Small, Medium), demonstrating the generality and scalability of our approach.

2. SAE-Track: Getting a Continual Series of SAEs

2.1. Preliminaries: Sparse Autoencoders

We follow the formulation in (Bricken et al., 2023; Templeton et al., 2024), where $\mathbf{x} \in \mathbb{R}^D$ denotes residual stream activations ($\mathbb{R}^D$ represents the **activation space**). This space is decomposed into $\mathbb{R}^F$ (defined as **feature space**), where F is the dictionary size of the sparse autoencoder.

The SAE reconstructs activations as:

$$\widehat{\mathbf{x}} = \mathbf{b}^{\text{dec}} + \sum_{i=1}^{F} f_i(\mathbf{x}) \mathbf{W}^{\text{dec}}_{:,i}, \tag{1}$$

where $\mathbf{W}^{\text{dec}} \in \mathbb{R}^{D \times F}$ are decoder weights, $\mathbf{b}^{\text{dec}} \in \mathbb{R}^D$ are biases, and $f_i(\cdot)$ represents feature activations computed as:

$$f_i(\mathbf{x}) = \text{ReLU}\left(\mathbf{W}^{\text{enc}}_{i,:} \cdot (\mathbf{x} - c \cdot \mathbf{b}^{\text{dec}}) + b^{\text{enc}}_i\right). \tag{2}$$

Here, $\mathbf{W}^{\text{enc}} \in \mathbb{R}^{F \times D}$ are encoder weights, $\mathbf{b}^{\text{enc}} \in \mathbb{R}^F$ are biases, and $c \in \{0, 1\}$ is a constant determining whether the decoder bias is included in the input transformation.

The loss function $\mathcal{L}$ combines reconstruction error and L1 norm regularization:

$$\mathcal{L} = \mathbb{E}_{\mathbf{x}}\left[\|\mathbf{x} - \widehat{\mathbf{x}}\|_2^2 + \lambda \mathcal{L}_1\right], \tag{3}$$

where

$$\mathcal{L}_1 = \begin{cases} \sum_i f_i(\mathbf{x}) & \text{(unit norm decoder constraint)}, \\ \sum_i f_i(\mathbf{x}) \cdot \|\mathbf{W}^{\text{dec}}_{:,i}\|_2 & \text{(no decoder constraint)}. \end{cases} \tag{4}$$

2.1.1. Key Intuitions

SAEs are trained on activations that evolve incrementally during gradient descent. Leveraging this continuity enables

efficient feature extraction and reduces noise when analyzing feature evolution across checkpoints.

Formally, let $F^{(l,t)}$ denote the transformer model at layer l and step t, parameterized by $\Theta^{(<l,t)}$. The activation for token q in context $\mathcal{C}$ is:

$$\mathbf{x}^{(l,\mathcal{C},q,t)} = F^{(l,t)}(\mathcal{C}, q; \Theta^{(<l,t)}). \tag{5}$$

For simplicity, we might omit some of $(l, \mathcal{C}, q, t)$ in subsequent discussions.

Theorem 2.1 (Training-Step Continuity). *Assume (1) the gradient norm $\|\nabla_{\Theta^{(<l)}}\mathcal{L}(\Theta)\| \leq G$ is bounded, and (2) the function $F^{(l)}$ is Lipschitz continuous with respect to $\Theta^{(<l)}$, with constant L. If the learning rate satisfies $\eta < \frac{\epsilon}{LG}$, then the activations evolve incrementally:*

$$\left\|\mathbf{x}^{(l,t)} - \mathbf{x}^{(l,t-1)}\right\| < \epsilon. \tag{6}$$

The proof is provided in Appendix A. Although real-world training may deviate from this idealized assumption, activation continuity motivates our approach to efficiently track feature evolution using a continual series of SAEs.

2.1.2. Methodology: Recurrent Initialization

To efficiently track feature evolution across training checkpoints, we propose **SAE-Track**, a framework that leverages recurrent initialization to construct a continual series of SAEs. Specifically:

- Each SAE[k] is initialized with the parameters of the previously trained SAE[$k-1$], ensuring smooth transitions and preserving continuity in SAE parameter.
- The process begins with SAE[1], which is randomly initialized and trained on activations from the first checkpoint (checkpoint[1]). Subsequent SAEs are then trained sequentially using activations from their respective checkpoints.

As illustrated in Fig. 1, this method ensures that the decoder weights evolve incrementally across checkpoints, significantly reducing the training cost for subsequent SAEs—$\leq \frac{1}{20}$ of the initial training steps. Furthermore, it enables real-time training, where SAEs are trained as checkpoints become available, without requiring access to all checkpoints upfront. This means that SAE-Track can be trained in parallel with the training of LLMs, enabling real-time interpretation and supervision throughout the training process. It also maintains the characteristics of normally trained SAEs, ensuring that the learned representations are consistent with our commonly used approach (see Appendix F).

SAE-Track provides an efficient and systematic approach to analyze feature dynamics throughout the training process. Based on the SAE series generated by SAE-Track, we can study the semantic evolution of features (Sec. 3), examine their formation from a geometric perspective (Sec. 4), and analyze how features undergo directional changes (Sec. 5).

3. Semantic Evolution of Features

In this section, we examine the features in the SAE series generated by SAE-Track and analyze the patterns of semantic evolution exhibited by these features.

Features extracted via SAEs are categorized into two types based on their activation behavior. We will discuss their behavior in detail after providing the following definitions:

Definition 3.1 (Token-Level Feature). *A **token-level feature** predominantly activates for a specific token, such as "century."*

Definition 3.2 (Concept-Level Feature). *A **concept-level feature** activates across a set of tokens that are semantically related to a broader concept. For instance, "authentication" and "getRole()" may activate for the concept "user authentication."*

Token-level features exist at all checkpoints, while concept-level features gradually emerge during the LLM's learning process. Specifically, the evolution of features can be described in three stages:

- **Initialization and Warmup.** Token-level features are present from the beginning, while other features remain as noise. At this stage, features lack meaningful associations beyond individual tokens, similar to the phenomenon described in (Bricken et al., 2023).
- **Emergent Phase.** Concept-level features begin to emerge, representing abstract concepts, while token-level features persist in parallel. Meanwhile, noise features gradually vanish.
- **Convergent Phase.** Both token-level and concept-level features converge into interpretable states, with concept-level features exhibiting coherent and semantically meaningful groupings.

We examine the semantic behavior of specific features throughout the LLM learning process. (Dead features and ultra-low activation features are excluded from this analysis, as well as all subsequent mechanistic analyses, as discussed in Appendix B.) Three distinct patterns of feature transformation are observed, as illustrated in Table 1:

- **Maintaining.** Token-level features persist across checkpoints, maintaining consistent activations for the same token.
- **Shifting.** Token-level features transition to different token-level ones or evolve into concept-level features, reflecting the reorganization of representations during training. This shifting process is inevitable for some

	checkpoint 0		checkpoint 15–21		checkpoint 153 (final)
Maintaining 4/61632	1. ... relevant information? 2. for the collection of status information 3. the information generated	⇒	1. provide additional information about a response. 2. providing information on walking, cycling	⇒	1. use information received from other agencies. 2. granted access to personally identifiable information.
Grouping 4/36072	1. Railway infrastructures 2. civic coffers, infrastructural development, ... 3. infrastructural growth 4. 0090688-Kimberling1 5. Kim and Eminem ...	⇒	1. a compelling insight 2. The Bottom Line 3. ... and its uneasy ... 4. compelling page-turner 5. N, KM, AK and AM are employees of ...	⇒	1. address some of the most compelling questions ... 2. a credible source for ... 3. no credible reason to ... 4. a compelling proposition 5. serious and credible
Shifting [to concept-level] 4/30867	1. Cataldo and De Marchi 2. republic of Catalonia 3. ... paid to Cataldo, 4. Serpico and Cataldo, 5. Catalyst-Accelerated 6. Graduate Catalogs	⇒	1. this Catalan government 2. Frances Dunn. Louisa 3. the Catalan parliament 4. majority of Louisianans 5. revolutionary leader Louis de Saint-Just...	⇒	1. Miguel Aleman is located 2. remuneration from Luis 3. ... RTA), and Jose Fernando Covian – Nares 4. writer Luis Pardo 5. Fernando Torres scored
Shifting [to token-level] 4/40671	1. media is fueled by similar ignorance 2. He claims ignorance 3. either through ignorance or internet 4. showing your ignorance	⇒	1. (astNode.isFunction) 2. ta toute la fine graisse du dessus ... 3. analysis.PolynomialFunctionLagrangeFormTest) 4. le pot de graisse se trouvait	⇒	1. @prop Function is Horizontal – returns 2. commons.math.FunctionEvaluationExceptionTest) 3. fn{Function |String} 4. ::js_sys::Function, \n)

Table 1. **Feature Semantic Evolution Patterns.** Illustration of the three primary feature evolution patterns during training: **Maintaining**, where features consistently activate for specific tokens across checkpoints; **Grouping**, where previously noisy features gradually organize into structured semantic ones; and **Shifting**, where a token-level feature either transitions to another token-level feature or evolves into a concept-level feature. Since concept-level features do not exist at initialization, **Shifting** exclusively begins from token-level features. The notation "layer/feature index" refers to the layer (preceding the residual stream) and the specific feature highlighted in the examples, with all tracking conducted on **Pythia-410m-deduped**.

features, as discussed in Appendix E.

- **Grouping.** Previously noisy features gradually organize into structured semantic ones, forming distinct token- or concept-level features.

4. Analysis of Feature Formation

In this section, we analyze how features transition from noisy activations to meaningful representations throughout training. We formally define key concepts, track the evolution of feature regions, and propose a Progress Measure to quantitatively assess this process in both activation and feature spaces.

4.1. Understanding Feature Formation from a Geometric Perspective

Existing studies often emphasize the final state of training or assume that features are inherently monosemantic (Bricken et al., 2023; Templeton et al., 2024; Elhage et al., 2022). However, training a SAE at any model checkpoint reveals features that define separable regions in the activation space. While the specific properties of these features may vary across checkpoints, they can all be understood from a unified geometric perspective: they represent distinct regions within the activation space.

From this perspective, the role of the SAE is to identify and isolate these regions. Formally, the encoder for feature i can be expressed as:

$$f_i(\mathbf{x}) = \text{ReLU}\left(\widehat{\mathbf{W}}_i \cdot \mathbf{x} + \widehat{b}_i\right), \tag{7}$$

where $\widehat{\mathbf{W}}_i = \mathbf{W}^{\text{enc}}_{i,:}$ and $\widehat{b}_i = b^{\text{enc}}_i - c \cdot \mathbf{W}^{\text{enc}}_{i,:} \cdot \mathbf{b}^{\text{dec}}$. Using this, we formalize the "feature region" for feature i as follows:

The function $f_i(\mathbf{x})$ naturally divides the activation space into regions via the ReLU function, where $\widehat{\mathbf{W}}_i \cdot \mathbf{x} + \widehat{b}_i > 0$ defines a region for $\mathbf{x}$. However, this division ignores the impact of activation strength, which is critical for semantic fidelity. As noted by (Bricken et al., 2023), higher activation levels often indicate stronger associations with specific tokens or concepts. In Fig. 2 (left), a 2D toy example shows how activation levels refine these regions, enabling a more precise characterization:

Definition 4.1 (Feature Region with Activation Level). *A region corresponding to feature i with activation level*

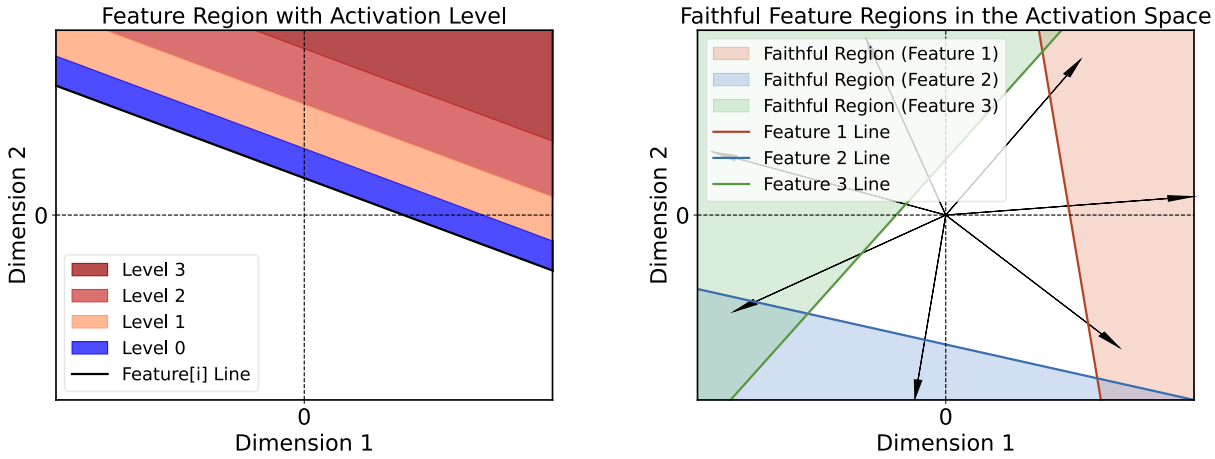

Figure 2. **Left:** A toy example illustrating feature regions with different activation levels in a 2D activation space. The colored regions represent varying activation intensities for a single feature, emphasizing the distinction between activation levels. **Right:** Faithful feature regions for three features, visualizing how features partition the activation space into semantically meaningful regions. This highlights the role of SAE in isolating and identifying these regions.

$[L, U)$ *is defined as:*

$$\mathcal{R}_i^{[L,U)} = \{\mathbf{x} \mid L \leq \left(\widehat{\mathbf{W}}_i \cdot \mathbf{x} + \widehat{b}_i\right) < U\}. \tag{8}$$

To assess semantic fidelity, we assume a threshold L_i beyond which a feature is considered semantically meaningful. This is formalized as:

Definition 4.2 (Faithful Feature Region). *A region that faithfully represents feature i is defined as:*

$$\mathcal{R}_i^{faithful} = \mathcal{R}_i^{[L_i,\infty)}, \tag{9}$$

where L_i is the threshold activation level required for semantic fidelity.

In Fig. 2 (right), a toy example demonstrates how the faithful regions of three features partition a 2D activation space. This example highlights the SAE's objective to identify these regions and provides insights into the geometric structure of the activation space.

Feature formation describes how datapoints with similar semantics converge into faithful feature regions in the activation space. To study this phenomenon, we track the evolution of datapoints within the same faithful feature region. Using the SAE at the final checkpoint, we define $\{\mathcal{R}_i^{\text{faithful}}[t = T_{\text{final}}]\}_{i=0}^{F-1}$ as the ground truth. Let $\mathcal{D}_i$ denote the set of datapoints that activate within $\mathcal{R}_i^{\text{faithful}}[T_{\text{final}}]$ at the final checkpoint, i.e.,

$$\mathcal{D}_i = \{(\mathcal{C}, q) \mid F^{(T_{\text{final}})}(\mathcal{C}, q; \Theta^{(T_{\text{final}})}) \in \mathcal{R}_i^{\text{faithful}}[T_{\text{final}}]\}, \tag{10}$$

where $\mathcal{C}$ represents the context and q denotes the token position within $\mathcal{C}$. The activation set of these datapoints at training step t is defined as:

$$\mathcal{A}_i^t = \{F^{(t)}(\mathcal{C}, q; \Theta^{(t)}) \mid (\mathcal{C}, q) \in \mathcal{D}_i\}. \tag{11}$$

Here, $\mathcal{A}_i^t$ represents the activations at checkpoint t for all datapoints in $\mathcal{D}_i$. Thus, studying feature formation involves analyzing the dynamics of $\{\mathcal{A}_i^t\}_{i=0}^{F-1}$ across training.

4.2. Visualization and Analysis

By tracking $\{\mathcal{A}_i^t\}_{i=0}^{F-1}$ across training steps t, we visualize the process of feature formation. Using UMAP (McInnes et al., 2020), we project the activation sets of various features across checkpoints (see Fig. 3, more detailed below). Datapoints with the top 25 feature activations are considered faithful, highlighting the dynamics of both token-level and concept-level features.

Initialization and Warmup Phase: Token-level feature datapoints are clusters, while concept-level feature datapoints remain scattered. In Fig. 3, Checkpoint 0, the initialized network shows tightly clustered token-level features. This arises because datapoints $(\mathcal{C}, q)$, corresponding to identical tokens in similar contexts $\mathcal{C}$, produce highly similar activations when passed through a transformer F with randomized parameters Θ_{rand}. The similarity is driven by shared tokens and repetitive contexts. In contrast, concept-level features remain scattered, as abstraction and generalization across related tokens do not occur in a randomized transformer. This phase reflects the early stage of feature development, dominated by basic token-level associations and noise.

Emergent Phase: Concept-level features begin clustering.

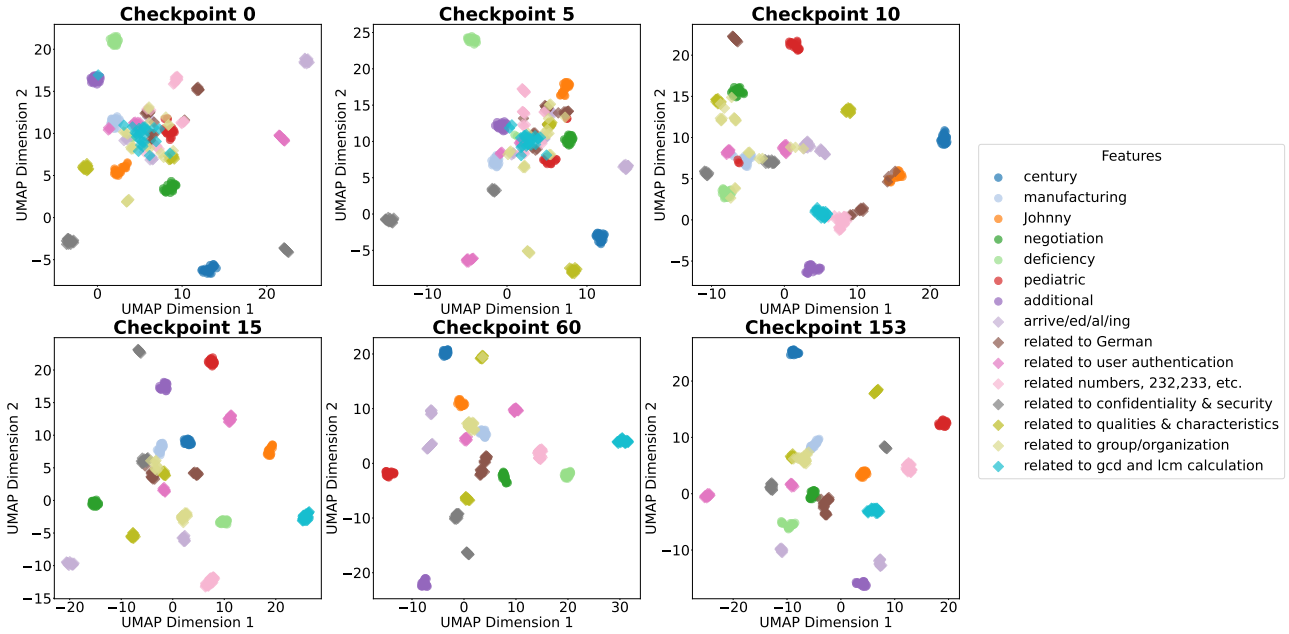

Figure 3. **UMAP Visualization.** UMAP illustrates the evolution of activation sets for various features across **Pythia-410m-deduped** checkpoints, with each colored point representing a datapoint associated with a distinct feature. Circular markers indicate token-level features, while diamond-shaped markers represent concept-level features. The visualization highlights the transition from random activations at the start of training (Checkpoint 0) to semantically coherent clusters at later stages (Checkpoint 153) and showcases the distinct dynamics of the two feature types.

As training progresses (Fig. 3, Checkpoints 5, 10, and 15), concept-level features transition from scattered points to cohesive clusters, reflecting the model's growing ability to represent concepts. Token-level features remain tightly clustered and stable throughout this phase.

Convergent Phase: Features stabilize into cohesive clusters. By Fig. 3, Checkpoints 60 and 153, both token-level and concept-level features are stable and well-formed, reflecting the model's fully developed ability to represent tokens and broader semantic concepts.

These visualizations at Fig. 3 across various checkpoints vividly illustrate the evolution of features, highlighting their transition from early random activations to semantically meaningful and well-defined clusters.

4.3. Progress Measure

It remains unclear whether feature formation represents a phase transition or a progressive process. To address this, we propose the **Feature Formation Progress Measure**, which quantifies the degree to which a feature becomes well-formed during training. This measure compares the similarity within semantic datapoints to a baseline derived from randomly sampled, unrelated datapoints.

Definition 4.3 (Feature Formation Progress Measure). *The metric $M_i(t)$ at training step t is defined as:*

$$M_i(t) = \overline{Sim}_{\mathcal{A}_i^t} - \overline{Sim}_{\mathcal{A}_{random}}, \tag{12}$$

where $\mathcal{A}_{random}$ represents a set of randomly sampled datapoints, and:

$$\overline{Sim}_{\mathcal{A}_i^t} = \frac{2}{|\mathcal{A}_i^t|(|\mathcal{A}_i^t|-1)} \sum_{\substack{x_k, x_j \in \mathcal{A}_i^t \\ j<k}} Sim(x_k, x_j), \tag{13}$$

$$\overline{Sim}_{\mathcal{A}_{random}} = \frac{2}{|\mathcal{A}_{random}|(|\mathcal{A}_{random}|-1)} \sum_{\substack{x_k, x_j \in \mathcal{A}_{random} \\ j<k}} Sim(x_k, x_j). \tag{14}$$

To extend the analysis to feature space, we define a corresponding measure:

$$M_i^{feature}(t) = \overline{Sim}_{\mathcal{F}_i^t} - \overline{Sim}_{\mathcal{F}_{random}}, \tag{15}$$

where:

$$\overline{Sim}_{\mathcal{F}_i^t} = \frac{2}{|\mathcal{F}_i^t|(|\mathcal{F}_i^t|-1)} \sum_{\substack{f_k, f_j \in \mathcal{F}_i^t \\ j<k}} Sim(f_k, f_j), \tag{16}$$

$$\overline{Sim}_{\mathcal{F}_{random}} = \frac{2}{|\mathcal{F}_{random}|(|\mathcal{F}_{random}|-1)} \sum_{\substack{f_k, f_j \in \mathcal{F}_{random} \\ j<k}} Sim(f_k, f_j). \tag{17}$$

Here, $\mathcal{F}_i^t$ represents the feature set of datapoints encoded by the SAE encoder at training step t, while $\mathcal{F}_{random}$ denotes

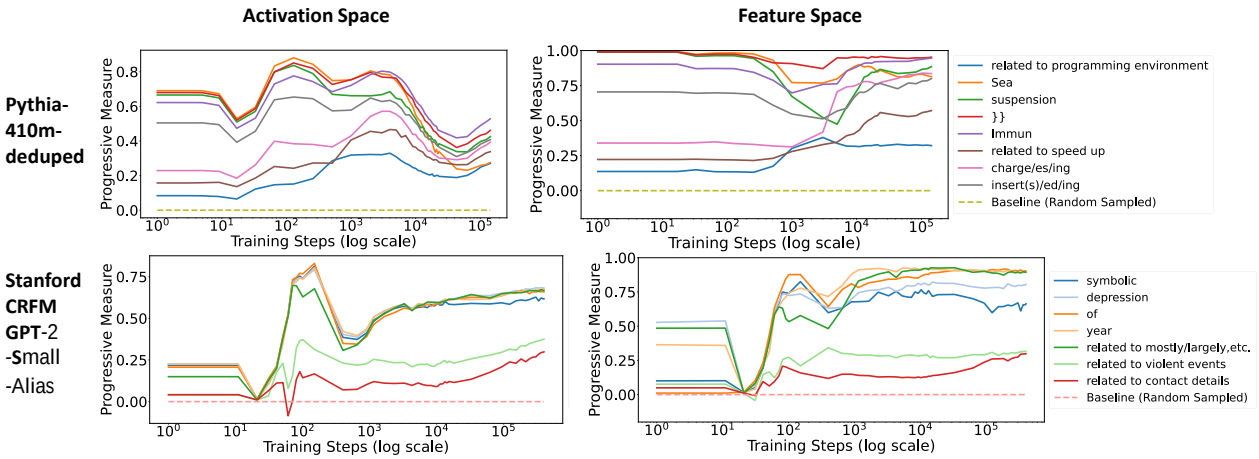

Figure 4. Progress Measure of activation space (**Left**) and feature space (**Right**) for **Pythia-410m-deduped** (**Top**) and **Stanford CRFM GPT-2 Small Alias** (**Bottom**) across training steps (log scale). For discussion of the glitch in Stanford CRFM GPT-2 Small Alias, see Appendix I.

the feature set for randomly sampled datapoints encoded in the same manner. By incorporating the feature space, this measure provides a finer-grained perspective on how datapoints align with features, offering valuable insights into the process of feature formation.

$Sim(\cdot, \cdot)$ can be computed using various metrics, such as cosine similarity or Jaccard similarity. In Fig. 4, we employ cosine similarity to demonstrate the utility of the proposed Progress Measure in capturing the gradual formation of features. Experiments with alternative similarity measures (e.g., Jaccard similarity) yield consistent results, as detailed in Appendix G, validating the robustness of this metric.

Notably, our Progress Measure captures the dynamic evolution of token-level and concept-level features, offering a quantitative view on feature formation. This complements the qualitative insights discussed in Sec. 4.2. Also, this measure further reveals that token-level and concept-level features are not entirely distinct. There is a continuous spectrum from typical token-level to high-level concept-level features, with intermediates (such as weak concept-level features) existing between them, as detailed in Appendix C.

5. Analysis of Feature Drift

It remains obscure whether feature directions drift throughout training or remain fixed from early on. **Our study reveals that feature directions initially exhibit significant drift, continue to drift even after features are considered "formed," and ultimately stabilize to their final state.** A feature is considered *formed* once it gains semantic meaning, which typically stabilizes its semantic association. However, our analysis shows that directional drift persists during training, reflecting ongoing refinements in the feature geometry before reaching stability.

5.1. Decoder Vector Evolution

Our analysis examines the evolution of decoder vectors $\{\mathbf{W}^{\text{dec}}_{:,i}\}_{i=0}^{F-1}$, which represent an overcomplete basis for the activation space. These vectors define the geometric representation of each feature and its contribution to reconstructing the activations. Following (Templeton et al., 2024), the direction of a feature i is defined as $\frac{\mathbf{W}^{\text{dec}}_{:,i}}{\left\|\mathbf{W}^{\text{dec}}_{:,i}\right\|}$.

To study the evolution of feature directions, we calculate the cosine similarity between decoder vectors at different training checkpoints. This quantifies how closely the directions of features at time t align with their final state at $t = \text{final}$.

Our analysis uses two complementary perspectives. Fig. 5(a) provides a checkpoint-centric view, summarizing the cosine similarity of all features at a given training time relative to their final state. This perspective offers a global snapshot of the model's progress in refining feature directions, revealing that feature directions in LLMs do not remain static during training. Instead, most features exhibit significant drift and gradually align with their final state as training progresses.

In contrast, Fig. 5(b) adopts a feature-centric view, illustrating how the similarity of a specific feature with its final state evolves across all training checkpoints. This visualization shows that the similarity initially remains relatively stable, then experiences a sudden increase during training, and gradually transitions into a plateau as it approaches the end. These trends align with the three phases we previously identified: *Initialization & Warmup*, *Emergent*, and *Convergent*. Together, these two perspectives complement each other, providing consistent yet distinct insights into the

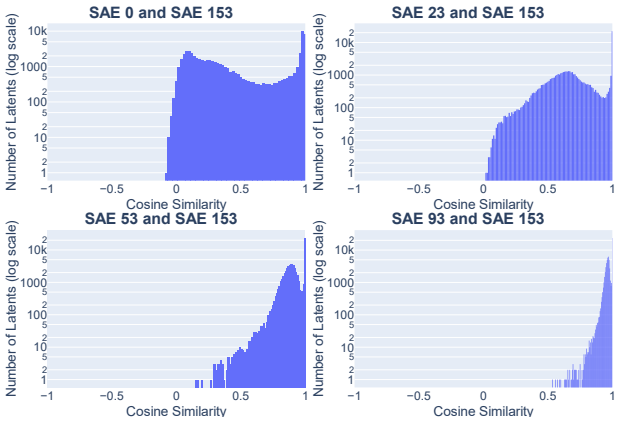

(a) Distribution of cosine similarity between decoder vectors at intermediate training checkpoints and the final checkpoint.

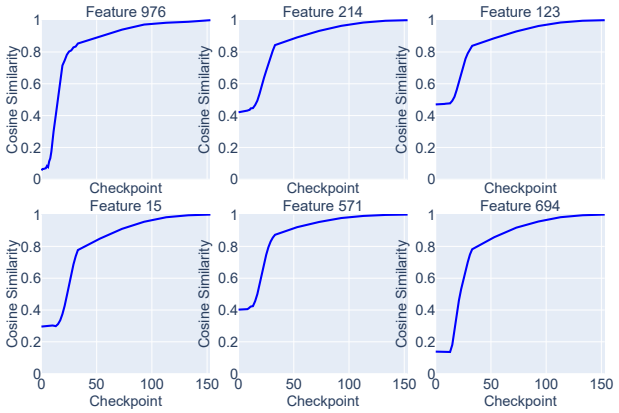

(b) Cosine similarity progression for sampled features across training checkpoints. Each subplot traces how individual features progressively approach their final direction.

Figure 5. **Decoder Vector Evolution.** Distribution and progression of cosine similarity between decoder vectors at intermediate checkpoints and their final state, illustrating both global alignment trends and individual feature dynamics throughout training. Conducted on **Pythia-410m-deduped**.

directional changes of features during training.

5.2. Trajectory Analysis

Building on the analysis of decoder vector evolution, we now examine feature trajectories to gain a deeper understanding of how features evolve across training checkpoints. By distinguishing the phases before and after a feature gains semantic meaning, we can better understand the relationship between directional drift and feature formation. This distinction highlights how drift persists even after feature formation, providing insights into the continuous adjustments in the feature space throughout training.

Definition 5.1 (Feature Trajectory). *Let* $\mathbf{W}_{:,i}^{dec}[t]$ *denote the decoder vector for feature* i *at training checkpoint* t*, where* $t \in \{1, \ldots, T_{final}\}$*. The trajectory of feature* i *is*

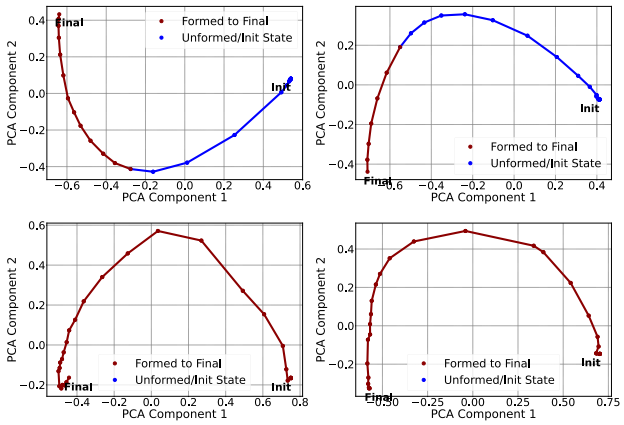

Figure 6. **Feature Trajectories.** Trajectories of decoder vectors represent the directional change of features across training checkpoints. "Dark red" indicates features that are considered "formed," i.e., they have gained semantic meaning and generally remain stable semantic meaning until the final state. "Blue" indicates features that are still unformed or in the initial stage. Conducted on **Pythia-410m-deduped**.

defined as:

$$\mathcal{J}_i = \left\{ \mathbf{W}_{:,i}^{dec}[1], \mathbf{W}_{:,i}^{dec}[2], \ldots, \mathbf{W}_{:,i}^{dec}[T_{final}] \right\}. \tag{18}$$

A feature is considered formed once it gains and stabilizes in semantic meaning. This means that trajectories exhibiting ("maintaining") behavior are always in the formed state, whereas those exhibiting ("shifting") or ("grouping") behaviors transition into the formed state later during training and remain in this state until the final checkpoint.

Fig. 6 illustrates that a feature would continue to drift even after gaining semantic meaning and considered formed, unveiling the dynamic relationship between directional drift and feature formation.

6. Conclusion

In this paper, we conduct a comprehensive mechanistic analysis of feature evolution in LLMs during training: (1) We propose SAE-Track, a novel method for obtaining a continual series of SAEs across training checkpoints, enabling efficient and stable feature tracking. (2) We mechanistically investigate feature formation and develop a progress measure for it, tracking the progression of features from noise to semantic fidelity. (3) We analyze feature drift, showing that feature directions initially exhibit significant adjustments and continue to drift even after features gain semantic meaning, before ultimately stabilizing at the final checkpoint. Our work provides a detailed understanding of how features evolve throughout training and lays the foundation for future studies. A more detailed discussion on its broader impact on this field, as well as potential future research directions, is provided in Appendix J.

Impact Statement

This paper presents work whose goal is to advance the field of Machine Learning. There are many potential societal consequences of our work, none which we feel must be specifically highlighted here.

References

Balagansky, N., Maksimov, I., and Gavrilov, D. Mechanistic permutability: Match features across layers, 2024.

Biderman, S., Schoelkopf, H., Anthony, Q. G., Bradley, H., O'Brien, K., Hallahan, E., Khan, M. A., Purohit, S., Prashanth, U. S., Raff, E., et al. Pythia: A suite for analyzing large language models across training and scaling. In *International Conference on Machine Learning*, pp. 2397–2430. PMLR, 2023.

Bricken, T., Templeton, A., Batson, J., Chen, B., Jermyn, A., Conerly, T., Turner, N., Anil, C., Denison, C., Askell, A., et al. Towards monosemanticity: Decomposing language models with dictionary learning. *Transformer Circuits Thread*, 2, 2023.

Chalnev, S., Siu, M., and Conmy, A. Improving steering vectors by targeting sparse autoencoder features, 2024.

Connor Kissane, robertzk, Arthur Conmy, and Neel Nanda. Saes (usually) transfer between base and chat models, 2024.

Cunningham, H., Ewart, A., Riggs, L., Huben, R., and Sharkey, L. Sparse autoencoders find highly interpretable features in language models, 2023.

Elhage, N., Hume, T., Olsson, C., Schiefer, N., Henighan, T., Kravec, S., Hatfield-Dodds, Z., Lasenby, R., Drain, D., Chen, C., et al. Toy models of superposition. *arXiv preprint arXiv:2209.10652*, 2022.

Engels, J., Liao, I., Michaud, E. J., Gurnee, W., and Tegmark, M. Not all language model features are linear. *arXiv preprint arXiv:2405.14860*, 2024.

Farrell, E., Lau, Y.-T., and Conmy, A. Applying sparse autoencoders to unlearn knowledge in language models, 2024.

Gao, L., Biderman, S., Black, S., Golding, L., Hoppe, T., Foster, C., Phang, J., He, H., Thite, A., Nabeshima, N., Presser, S., and Leahy, C. The Pile: An 800gb dataset of diverse text for language modeling. *arXiv preprint arXiv:2101.00027*, 2020.

Gokaslan, A., Cohen, V., Pavlick, E., and Tellex, S. Openwebtext corpus. http://Skylion007.github.io/OpenWebTextCorpus, 2019.

Jack Lindsey, Adly Templeton, Jonathan Marcus, Thomas Conerly, Joshua Batson, and Christopher Olah. Sparse crosscoders for cross-layer features and model diffing. *Transformer Circuits Thread*, 2024.

Joseph Bloom, C. T. and Chanin, D. Saelens. https://github.com/jbloomAus/SAELens, 2024.

Karamcheti, S., Orr, L., Bolton, J., Zhang, T., Goel, K., Narayan, A., Bommasani, R., Narayanan, D., Hashimoto, T., Jurafsky, D., Manning, C. D., Potts, C., Ré, C., and Liang, P. Mistral - a journey towards reproducible language model training, 2021. URL https://github.com/stanford-crfm/mistral.

Lan, M., Torr, P., Meek, A., Khakzar, A., Krueger, D., and Barez, F. Sparse autoencoders reveal universal feature spaces across large language models, 2024.

Li, Y., Li, Y., and Risteski, A. How do transformers learn topic structure: Towards a mechanistic understanding. In *International Conference on Machine Learning*, pp. 19689–19729. PMLR, 2023.

Li, Y., Michaud, E. J., Baek, D. D., Engels, J., Sun, X., and Tegmark, M. The geometry of concepts: Sparse autoencoder feature structure, 2024.

Lin, J. Training sparse autoencoders on language models. https://github.com/hijohnnylin/mats_sae_training, 2024.

Liu, D., Wang, S., Ren, J., Wang, K., Yin, S., Deng, H., and Zhang, Q. Trap of feature diversity in the learning of mlps, 2022. URL https://arxiv.org/abs/2112.00980.

McDougall, C. SAE Visualizer. https://github.com/callummcdougall/sae_vis, 2024.

McInnes, L., Healy, J., and Melville, J. Umap: Uniform manifold approximation and projection for dimension reduction, 2020.

Nanda, N. and Bloom, J. Transformerlens. https://github.com/TransformerLensOrg/TransformerLens, 2022.

Nanda, N., Chan, L., Lieberum, T., Smith, J., and Steinhardt, J. Progress measures for grokking via mechanistic interpretability. *arXiv preprint arXiv:2301.05217*, 2023.

Olsson, C., Elhage, N., Nanda, N., Joseph, N., DasSarma, N., Henighan, T., Mann, B., Askell, A., Bai, Y., Chen, A., et al. In-context learning and induction heads. *arXiv preprint arXiv:2209.11895*, 2022.

Park, K., Choe, Y. J., and Veitch, V. The linear representation hypothesis and the geometry of large language models. *arXiv preprint arXiv:2311.03658*, 2023.

Qian, C., Zhang, J., Yao, W., Liu, D., Yin, Z., Qiao, Y., Liu, Y., and Shao, J. Towards tracing trustworthiness dynamics: Revisiting pre-training period of large language models. *arXiv preprint arXiv:2402.19465*, 2024.

Radford, A., Wu, J., Child, R., Luan, D., Amodei, D., Sutskever, I., et al. Language models are unsupervised multitask learners. *OpenAI blog*, 1(8):9, 2019.

Taras Kutsyk, Tommaso Mencattini, C. F. Do sparse autoencoders (saes) transfer across base and finetuned language models?, 2024.

Templeton, A., Conerly, T., Marcus, J., Lindsey, J., Bricken, T., Chen, B., Pearce, A., Citro, C., Ameisen, E., Jones, A., et al. Scaling monosemanticity: extracting interpretable features from claude 3 sonnet, transformer circuits thread, 2024.

Yin, Q., Leong, C. T., Zhang, H., Zhu, M., Yan, H., Zhang, Q., He, Y., Li, W., Wang, J., Zhang, Y., and Yang, L. Direct preference optimization using sparse feature-level constraints, 2024.

A. Detailed Derivation of the Training-Step Continuity Theorem

Assume the conditions hold. Using a first-order Taylor expansion:

$$\mathbf{x}^{(l,t)} \approx \mathbf{x}^{(l,t-1)} + \frac{\partial F^{(l)}}{\partial \Theta^{(<l)}}\Big|_{\Theta^{(<l,t-1)}} \cdot (\Theta^{(<l,t)} - \Theta^{(<l,t-1)}). \tag{19}$$

Substituting the gradient descent update $\Theta^{(<l,t)} - \Theta^{(<l,t-1)} = -\eta \nabla_{\Theta^{(<l)}} \mathcal{L}(\Theta^{(t-1)})$, we have:

$$\mathbf{x}^{(l,t)} \approx \mathbf{x}^{(l,t-1)} - \eta \frac{\partial F^{(l)}}{\partial \Theta^{(<l)}}\Big|_{\Theta^{(<l,t-1)}} \cdot \nabla_{\Theta^{(<l)}} \mathcal{L}(\Theta^{(t-1)}). \tag{20}$$

Taking norms and applying the bounds on $\frac{\partial F^{(l)}}{\partial \Theta^{(<l)}}$ and $\nabla_{\Theta^{(<l)}} \mathcal{L}(\Theta)$:

$$\left\| \mathbf{x}^{(l,t)} - \mathbf{x}^{(l,t-1)} \right\| \leq \eta L G. \tag{21}$$

With $\eta < \frac{\epsilon}{LG}$, this ensures:

$$\left\| \mathbf{x}^{(l,t)} - \mathbf{x}^{(l,t-1)} \right\| < \epsilon, \tag{22}$$

proving continuous activation changes over training steps.

This derivation supports the Training-Step Continuity Theorem by bounding activation changes through Lipschitz continuity and gradient norms. The result highlights the incremental and stable evolution of activations during training.

B. Dead Features and Ultra-Low Activation Features

In our analysis, we exclude two categories of features that fail to contribute meaningful information during training:

- **Dead Features**: These are features that do not activate on any datapoint. Such features are entirely uninformative and irrelevant to the our study.
- **Ultra-Low Activation Features**: Features with extremely low activation densities or values are also excluded. While not strictly inactive, these features exhibit negligible activations that render them semantically meaningless. This filtering is consistent with prior observations in (Bricken et al., 2023), which identify such low-activation features as non-contributive.

By filtering these two types of features, we focus on those that exhibit meaningful activations and contribute to the evolving structure of the activation space, enabling a clearer study of feature dynamics.

C. Weak Concept-Level Features and a Potentially Finer-Grained Concept Spectrum

Concept-level features with limited variants, such as morphological features corresponding to suffixes (e.g., *-ed*, *-ing*), can be considered weak concept-level features. For instance, a feature might primarily activate for 10 occurrences of *-ing* and 15 of *-ed*, leading to repeated pairings during similarity calculations. This repetition often inflates similarity scores in similarity-based metrics, despite these features being fundamentally identical in nature to typical concept-level features.

	Feature Activation
Weak Concept-Level Features 4/5464	1. being utilized in mass drug administration campaigns 2. by utilizing SEO tips for beginners 3. utilizing toys around the house like ... 4. may be selected and utilized to record other bodily ionic ... 5. Shelton then utilized a technique whereby ... 6. so that it may be utilized by the specific print engine 7. develop and utilize the seven ESI skills 8. jargon will be utilized which is identified ... 9. to the procedure to be utilized in determining ... 10. most processes have utilized the blade outer ... 11. it is utilized by the over 1, ... 12. the system can be utilized to significantly ... 13. likely to be utilized in the arithmetic unit 14. if you aren't utilizing social networking ... 15. are utilized by all levels of fly ... 16. to make their websites utilized more effectively 17. help your employees choose and utilize their benefits 18. fans on all headers utilize high-amperage 19. none of it utilized multiple threads ...

Table 2. **Weak Concept-Level Features.**

At the start of training, datapoints corresponding to weak features often form multiple separate clusters in the activation space. However, this clustering is a superficial phenomenon that reflects redundancy rather than meaningful semantic coherence. Only via training does the model gradually learn to organize these datapoints into a single cohesive feature.

As discussed in the main paper, there may exist a continuous spectrum and a hierarchical structure in feature levels, along with potential different geometric properties in the activation space and different training dynamics. We frame this as the **Concept Spectrum Hypothesis**, which suggests the feature hierarchy from lower-level token-based representations to higher-level abstract concepts. A formal quantitative characterization of this hierarchy is beyond the scope of this work and is **left for future research**.

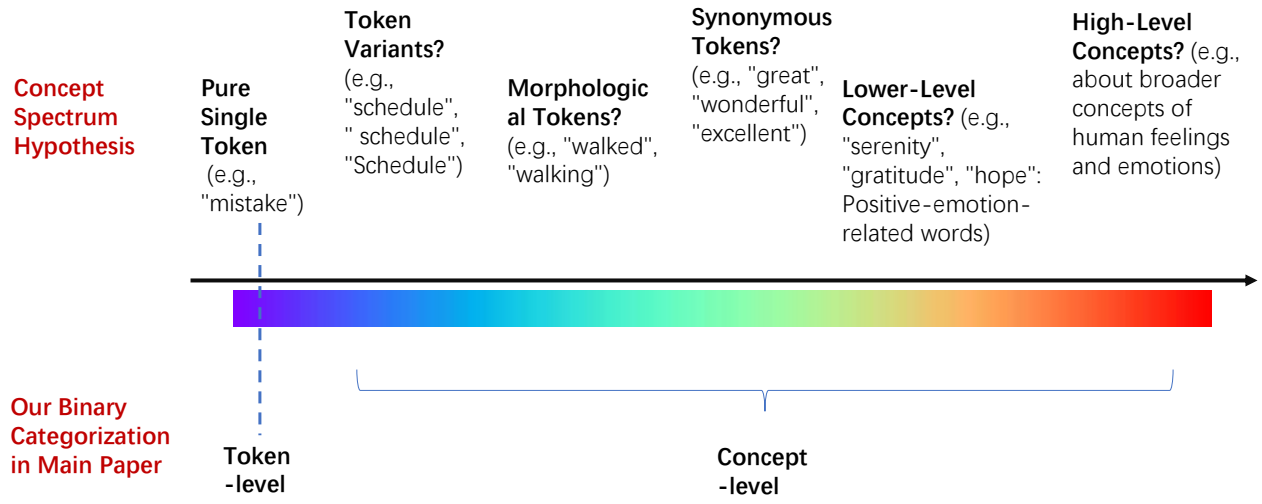

Figure 7. **Illustration of the Concept Spectrum Hypothesis.** This figure illustrates the hierarchy from pure token-level features to higher-level concept-level features. The spectrum represents a continuous hierarchy of learned features, offering a potential refinement beyond the binary categorization discussed in our main paper.

D. Polysemous Token-Level Features.

For polysemous tokens—tokens with multiple meanings—the corresponding token-level features may initially activate without capturing any semantic distinctions. During the early training phase, these features are primarily activated based on token identity alone. However, as training progresses and the model learns to incorporate semantics, these features sometimes degrade to represent only the most prominent meaning of the token. This degradation reflects the model's learning process, where it begins to understand and refine what a token-level feature truly represents, prioritizing the most frequent or contextually significant meaning.

	checkpoint 0		**checkpoint 15–21**		**checkpoint 153 (final)**
Degradation of Polysemy 4/20242	1. hold firm and cherish 2. issued a firm threat 3. oil firm for decades 4. absolutely firm and ... 5. landscape design firm 6. the US firm is not...	⇒	1. the US firm is not... 2. brokerage firm CPNA 3. landscape design firm 4. no organization or firm ... 5. as a firm, purple-blue... 6. have a firm mattress	⇒	1. North Carolina-based firm 2. prestigious law firm 3. the firm offers probate 4. from the law firm 5. policy of the firm 6. by leading US law firm,

Table 3. **Polysemous Token-Level Features.** Words in blue denote "resolute" or "solid," while green indicates "company" or "organization," highlighting the model's refinement of polysemous meanings during training.

E. The Challenge of Tracking the Semantics of Initial Features

One might expect that all (token-level) features observed during the initialization stage can be consistently tracked throughout training. However, this is not feasible due to several key reasons:

- **Emergent Phase Dynamics**: During the emergent phase, activations corresponding to initially distinct datapoints may overlap or merge, resulting in features that no longer align with their initial definitions.
- **Lack of Ideal Continual Steps**: There are no ideal continual training steps, as discussed in Theorem 2.1, which complicates the tracking of features across training, especially in stages where the checkpoints are sparsely distributed.
- **SAE Training Property**: SAE training can be viewed as selecting features from a large pool of possible features to explain the model activations (Templeton et al., 2024). Even when training SAEs twice on the same model activations and data, divergence in learned features can occur (Bricken et al., 2023). This selection process inherently introduces inconsistencies between initial and final features.
- **Shifting Phenomenon**: Unlike the initial checkpoint, where SAEs mainly produce token-level features, the final checkpoint SAEs are not constrained to token-level representations. As training progresses, features initially aligned to specific tokens may shift and evolve into other features. This transformation makes strict feature tracking across checkpoints impractical.
- **The Impact of Possible Feature Collapse:** See Discussion Appendix I.2 at Appendix I.

It is important to emphasize that SAE-Track is designed as a study tool rather than an engineering evaluation framework. The goal is to provide insights into feature dynamics, not to enforce strict feature-tracking consistency.

F. Implementation Details

Most experiments were conducted on a single NVIDIA A100 GPU. The implementation is built primarily upon open-source codebases (McDougall, 2024; Joseph Bloom & Chanin, 2024; Lin, 2024; Nanda & Bloom, 2022).

Models and Datasets: We use the Pythia-deduped models (Biderman et al., 2023) and Stanford CRFM Mistral (Karamcheti et al., 2021) for our experiments.

Pythia provides 154 checkpoints across training, with the checkpoints recorded at the following training steps:

$$[0, 1, 2, 4, 8, 16, 32, 64, 128, 256, 512] + \text{list(range(1000, 143000 + 1, 1000))}.$$

We conduct experiments on three Pythia scales: 160M, 410M, and 1.4B parameters, ensuring consistency across model sizes.

Stanford CRFM Mistral (Karamcheti et al., 2021) provides an open-source replication of the GPT-2 model (Radford et al., 2019), including five GPT-2 Small and five GPT-2 Medium models trained on the OpenWebText corpus (Gokaslan et al., 2019). Each model produces 609 checkpoints, recorded at the following training steps:

$$\begin{aligned}&\text{list(range(0, 100, 10))} + \text{list(range(100, 2000, 50))}\\&+ \text{list(range(2000, 20000, 100))} + \text{list(range(20000, 400000 + 1, 1000))}.\end{aligned}$$

Datasets used in training SAE-Track and conducting mechanistic experiments correspond to the datasets used during model training.

Stanford CRFM GPT-2 models use the OpenWebText corpus (Gokaslan et al., 2019), while Pythia models use the deduplicated version of the Pile dataset (Gao et al., 2020). The deduplicated Pile dataset ensures minimal repetition in the training data, aligning with the Pythia-deduped models.

SAEs Training: To efficiently train SAEs across multiple checkpoints, we employ a recurrent initialization scheme, which reuses the weights from the previous checkpoint to initialize the current SAE. The checkpoints for SAE training are selected based on an adaptive schedule:

$$S = \bigcup_{i=1}^{M} \bigcup_{j=0}^{n_i-1} (a_i + d_i \cdot j)\,, \quad \text{where } \begin{aligned}&M \text{ is the total number of segments,}\\&a_i \text{ is the starting value of the } i\text{-th segment,}\\&d_i \text{ is the step size of the } i\text{-th segment,}\\&n_i \text{ is the number of elements in the } i\text{-th segment,}\\&a_i = a_{i-1} + d_{i-1} \cdot n_{i-1} \text{ ensures continuity.}\end{aligned} \tag{23}$$

This piecewise linear schedule adapts the checkpoint density across training phases. In later training checkpoints, fewer checkpoints suffice as feature evolution slows, reducing computational costs while preserving representation quality. However, using all checkpoints or a denser selection can enhance tracking precision when needed.

Overtraining is applied to enhance feature representations, as recommended in (Bricken et al., 2023). By leveraging the recurrent initialization scheme, which reuses pretrained weights, convergence is significantly accelerated. Specifically, only $\leq \frac{1}{20}$ of the initial training tokens are required for subsequent SAEs, resulting in substantial computational savings.

A Training Example: Here we present an example trained on **Pythia-410M-Deduped**.

We follow the training schedule:

$$\text{list(range(33))} + \text{list(range(33, 153, 5))} \tag{24}$$

SAE[0] is trained using 300M tokens, while checkpoints 1–4 each use 5M tokens, and all remaining checkpoints use 15M tokens. The training details are illustrated in terms of overall loss, MSE loss, explained variance, and L_0 metric.

For comparison, we also train an SAE on the final LLM checkpoint, following the commonly used approach of training SAEs on a fixed checkpoint. The results show that SAE-Track-generated SAEs exhibit similar behavior to normally trained SAEs.

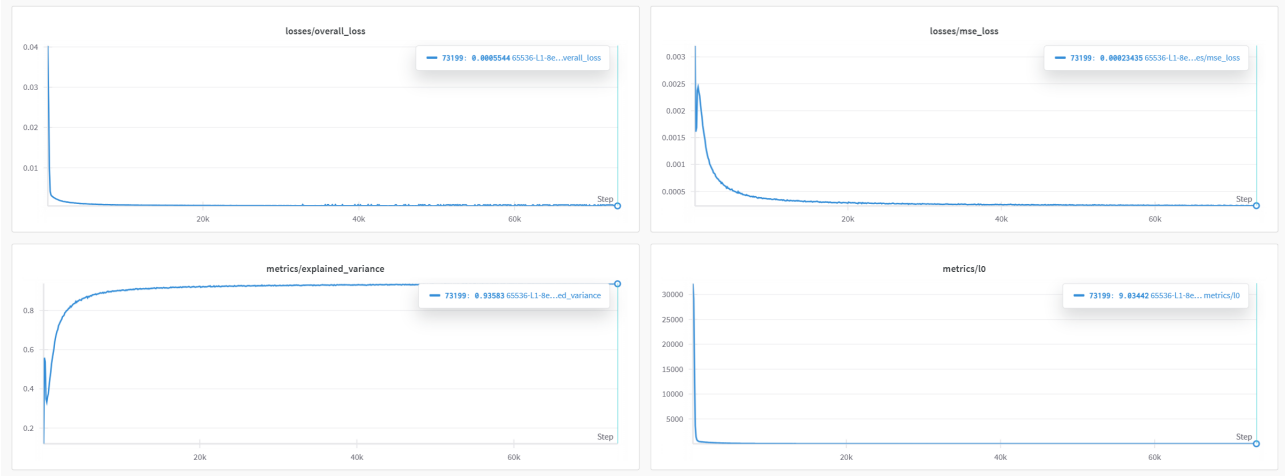

Figure 8. SAE[0] training, SAE-Track

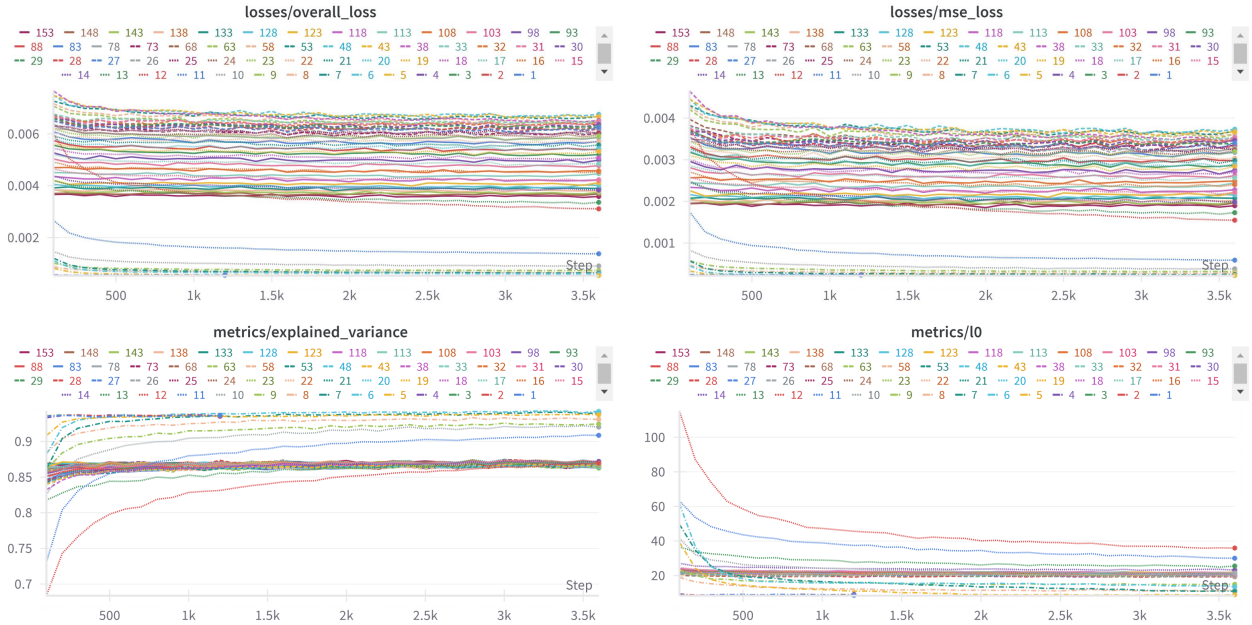

Figure 9. SAE[1]-SAE[153] training, SAE-Track

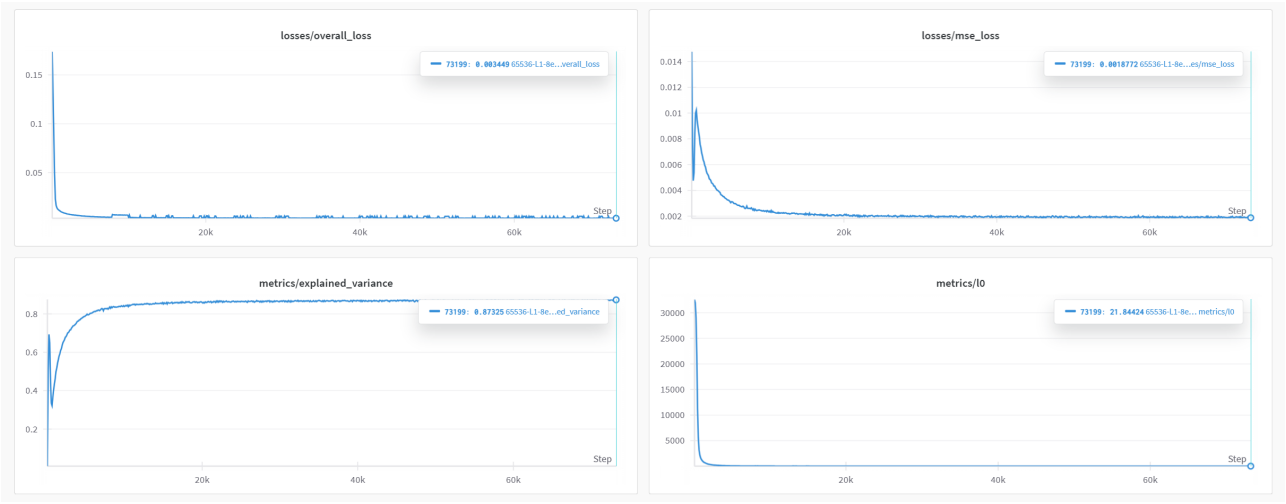

Figure 10. SAE trained (normally) on 153

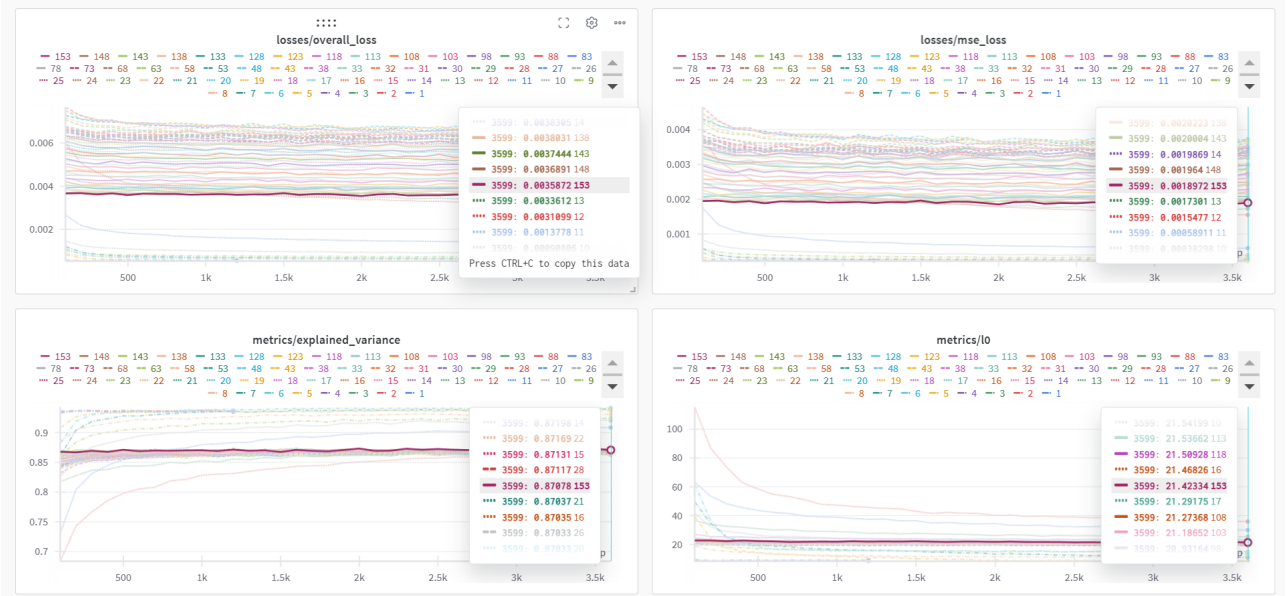

Figure 11. SAE[153](SAE-Track) share similar behavior of normally trained SAE on checkpoint 153

G. Different Similarity Metrics

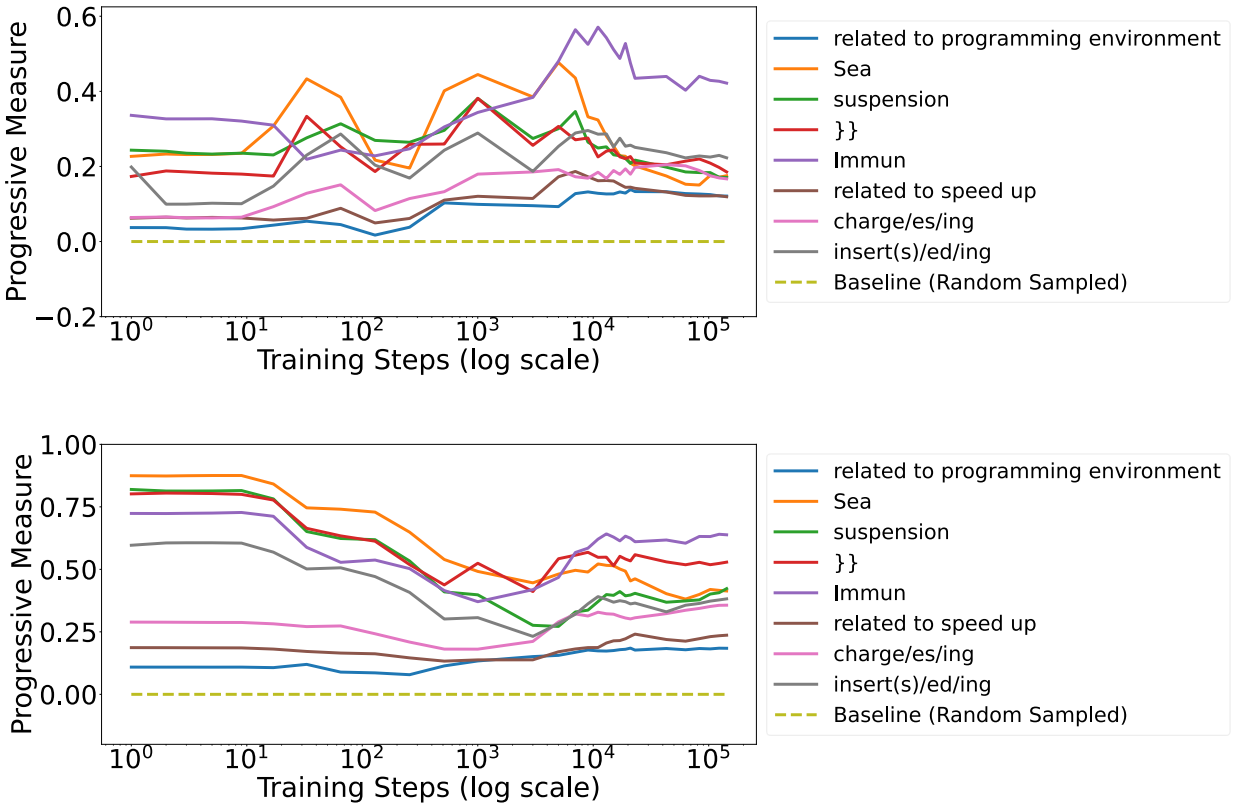

Figure 12. **Progress Measure using different similarity metrics.**Top: jaccard similarity for feature space, Bottom: weighted jaccard similarity for feature space. Conducted on **Pythia-410-Deduped**.

Our progress measure relies on the choice of similarity metrics. In the main text, we use cosine similarity; here, we extend the analysis by exploring additional metrics, as shown in Fig. 12. The results demonstrate that the overall trend remains consistent across different metrics. Specifically, token-level features exhibit relatively stable high values, while concept-level features gradually increase in similarity metric values as training progresses. Importantly, the choice of similarity metric does not significantly affect the overall analysis or conclusions.

Definitions of Similarity Metrics:

- **Cosine Similarity:** Cosine similarity, applied to the activation space with new datapoints, measures the angular similarity between two vectors $\mathbf{u}$ and $\mathbf{v}$. It is defined as:

$$\text{CosSim}(\mathbf{u}, \mathbf{v}) = \frac{\mathbf{u} \cdot \mathbf{v}}{\|\mathbf{u}\| \|\mathbf{v}\|}, \tag{25}$$

  where $\mathbf{u} \cdot \mathbf{v}$ denotes the dot product, and $\|\mathbf{u}\|$, $\|\mathbf{v}\|$ are the norms of the respective vectors.

- **Jaccard Similarity:** Jaccard similarity is applied to the sparse feature space. It converts each feature vector into a binary representation, indicating whether a feature is activated (1) or not (0), and calculates similarity as:

$$\text{Jaccard}(\mathbf{u}, \mathbf{v}) = \frac{|\mathbf{u}_{\text{binary}} \cap \mathbf{v}_{\text{binary}}|}{|\mathbf{u}_{\text{binary}} \cup \mathbf{v}_{\text{binary}}|}, \tag{26}$$

  where $\mathbf{u}_{\text{binary}}$ and $\mathbf{v}_{\text{binary}}$ are the binary representations of $\mathbf{u}$ and $\mathbf{v}$, respectively.

- **Weighted Jaccard Similarity:** Weighted Jaccard similarity extends Jaccard similarity by considering the magnitude of activations in the feature space. For two activation vectors $\mathbf{u}$ and $\mathbf{v}$, it is defined as:

$$\text{WeightedJaccard}(\mathbf{u}, \mathbf{v}) = \frac{\sum_i \min(u_i, v_i)}{\sum_i \max(u_i, v_i)}, \tag{27}$$

  where u_i and v_i are the activation values for feature i in $\mathbf{u}$ and $\mathbf{v}$, respectively.

Since Jaccard and Weighted Jaccard are more suitable for sparse vectors, and their meaning becomes less significant for non-sparse vectors, we restrict their use to the feature space. The overall trends presented in Fig. 12 demonstrate that the choice of metric does not substantially affect the study's conclusions.

H. Experiments on Different Models

H.1. Pythia of Different Scales

Below, we present results for **Pythia-160m-deduped, layer=4** and **Pythia-1.4b-deduped, layer=3**, trained on the residual stream before the specified layers. The figures include UMAP, progress measures, decoder cosine similarity, and trajectory analysis. These results align closely with those observed for **Pythia-410m-deduped, layer=4** in the main paper, highlighting the consistency of our results.

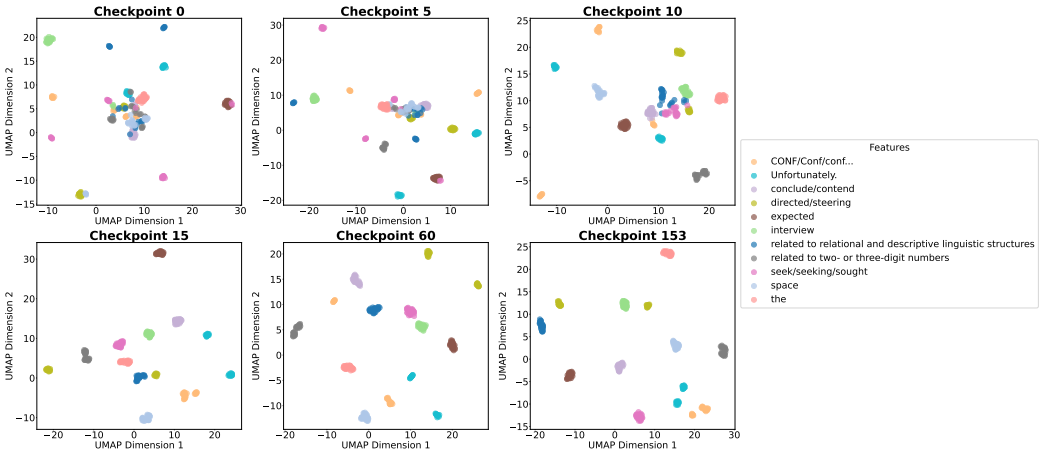

Figure 13. **UMAP for Pythia-160m-deduped.**

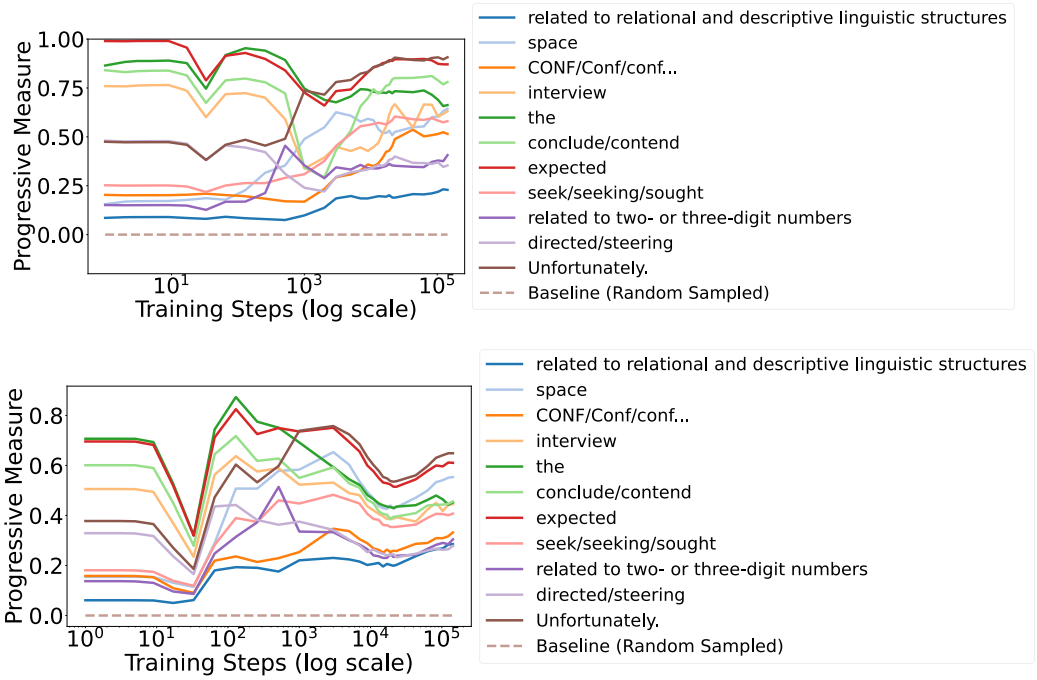

Figure 14. **Progress Measure for Pythia-160m-deduped.** The top represents the feature space, while the bottom represents the activation space.

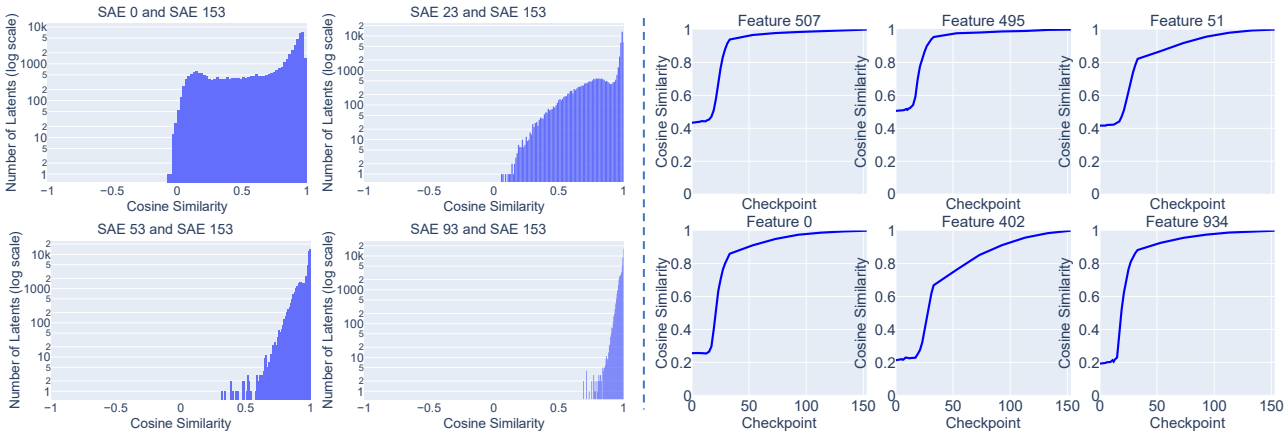

Figure 15. **Cosine Similarity for Pythia-160m-deduped.**

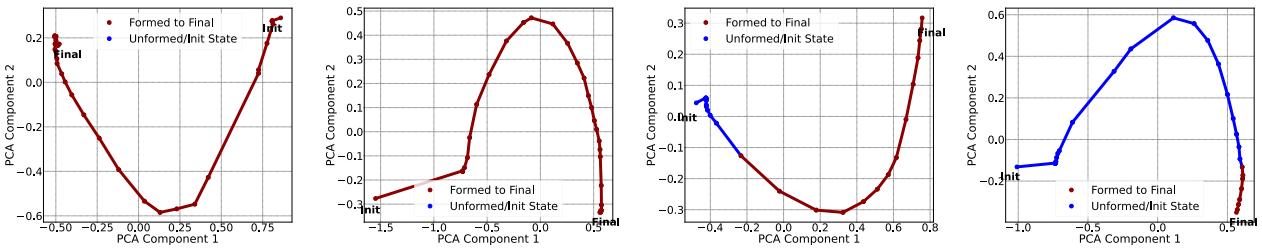

Figure 16. **Feature Trajectories for Pythia-160m-deduped.**

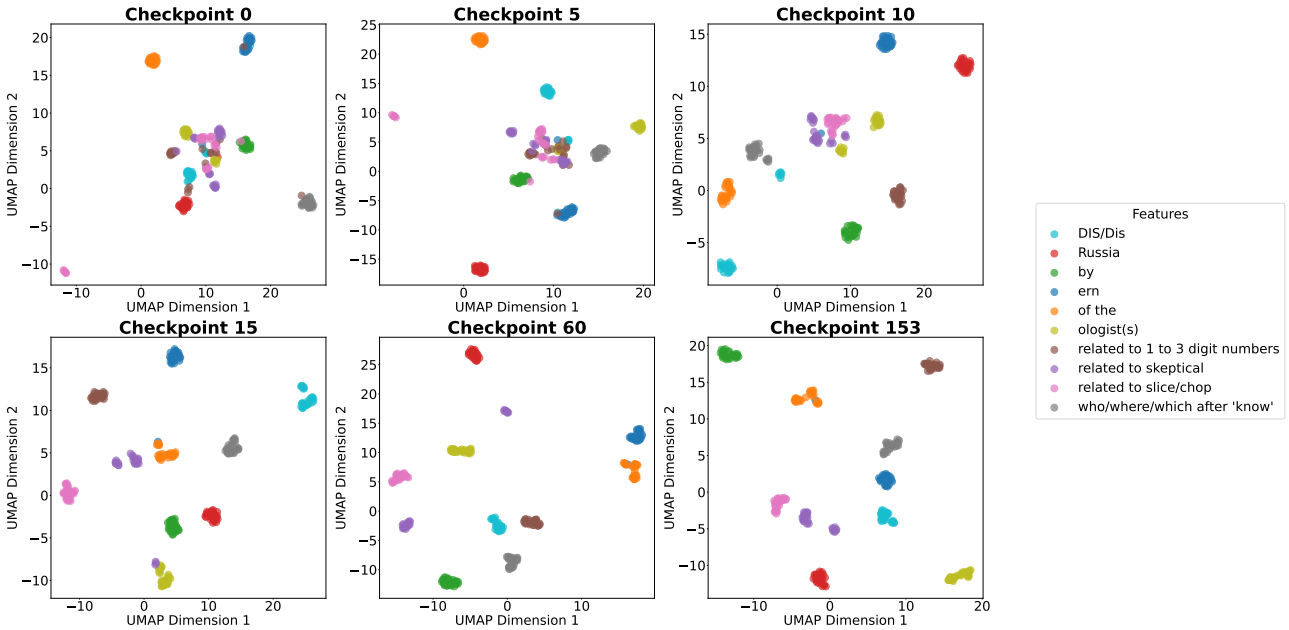

Figure 17. **UMAP for Pythia-1.4b-deduped.**

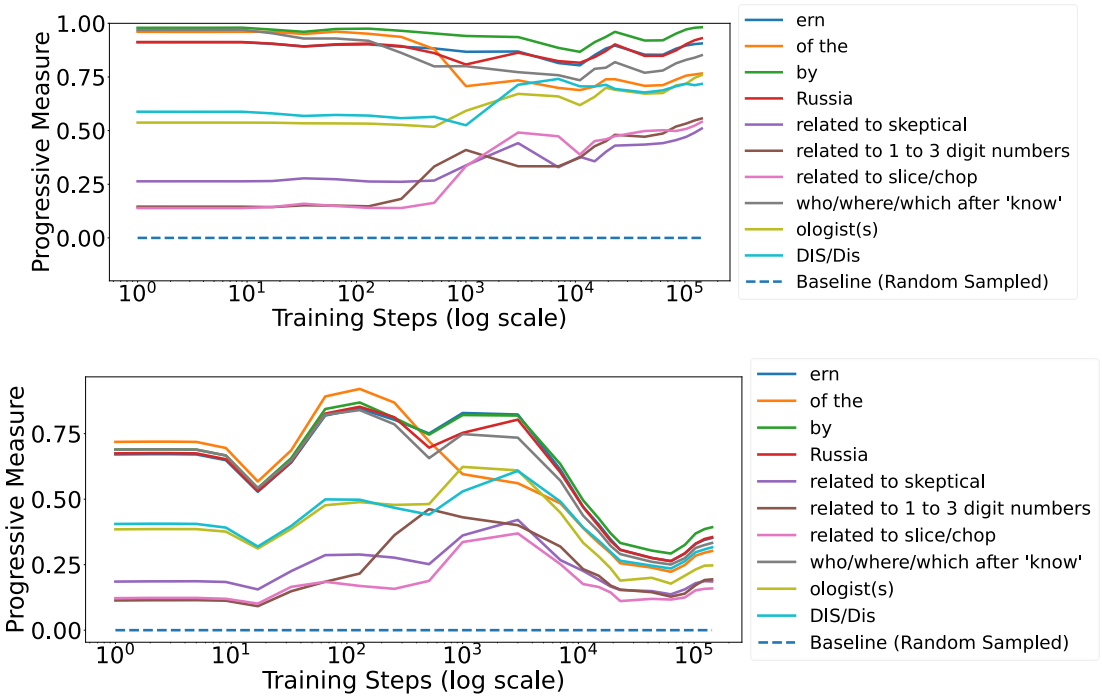

Figure 18. **Progress Measure for Pythia-1.4b-deduped.** The top represents the feature space, while the bottom represents the activation space.

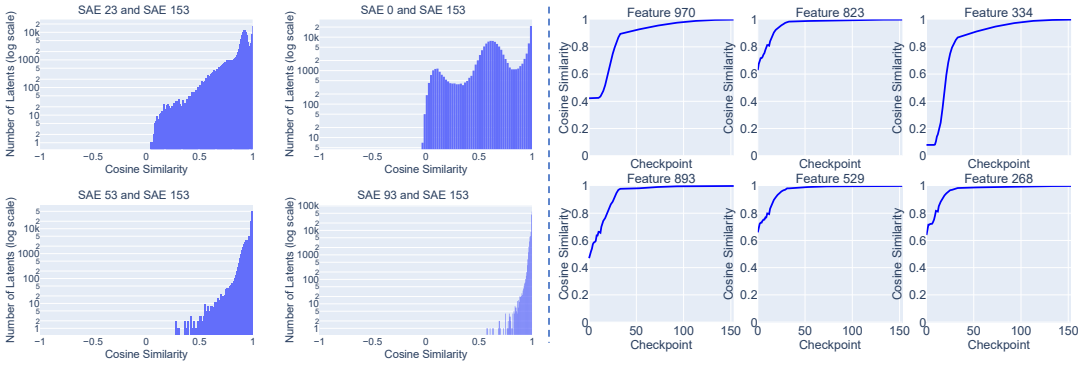

Figure 19. **Cosine Similarity for Pythia-1.4b-deduped.**

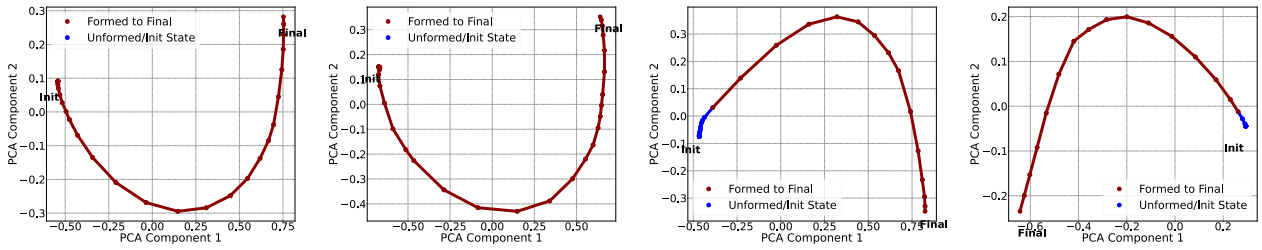

Figure 20. **Feature Trajectories for Pythia-1.4b-deduped.**

H.2. Stanford GPT2 of Different Scales

Below, we present results for **stanford-gpt2-small-a, layer=5** and **stanford-gpt2-medium-a, layer=6**, trained on the residual stream before the specified layers. The figures include UMAP, progress measures, decoder cosine similarity, and trajectory analysis.

The results are mainly consistent, except for the glitch observed in Stanford-GPT2-Small-A and the UMAP of initialization. The UMAP at initialization appears more diverged, which is related to both the initialization scheme and the model architecture. However, token-level features still exist at this stage. The glitch is further explained in Appendix I.

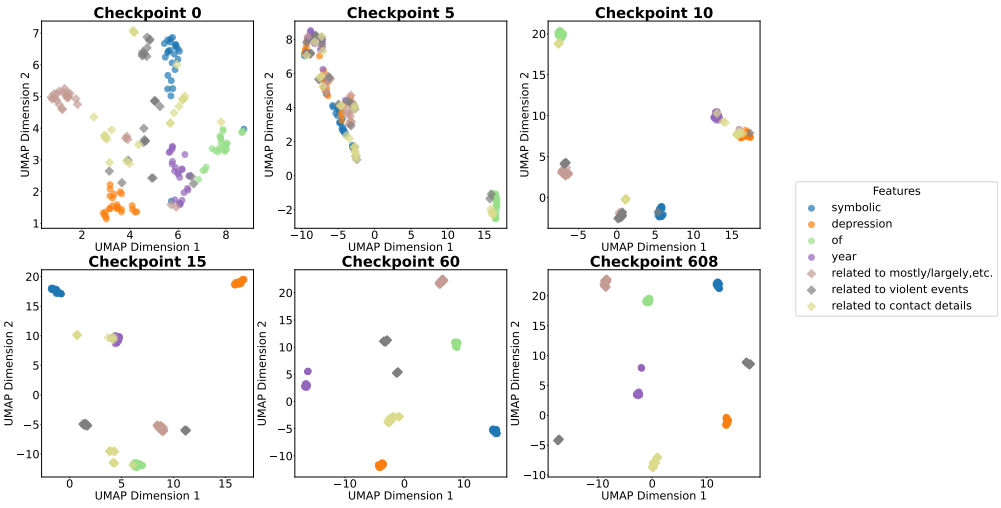

Figure 21. **UMAP for stanford-gpt2-small-a.**

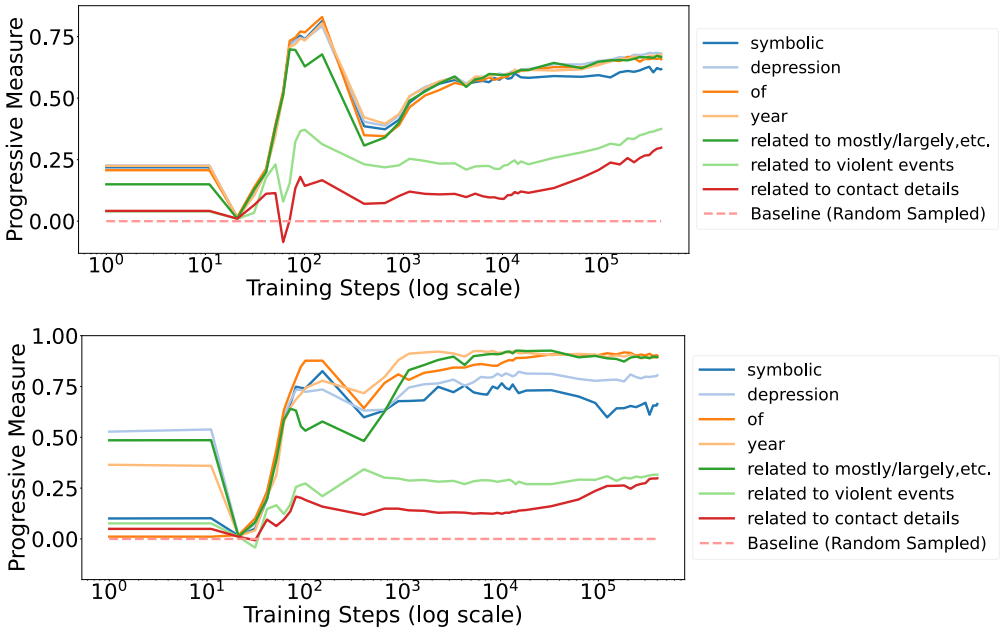

Figure 22. **Progress Measure for stanford-gpt2-small-a.** The top represents the activation space, while the bottom represents the feature space.

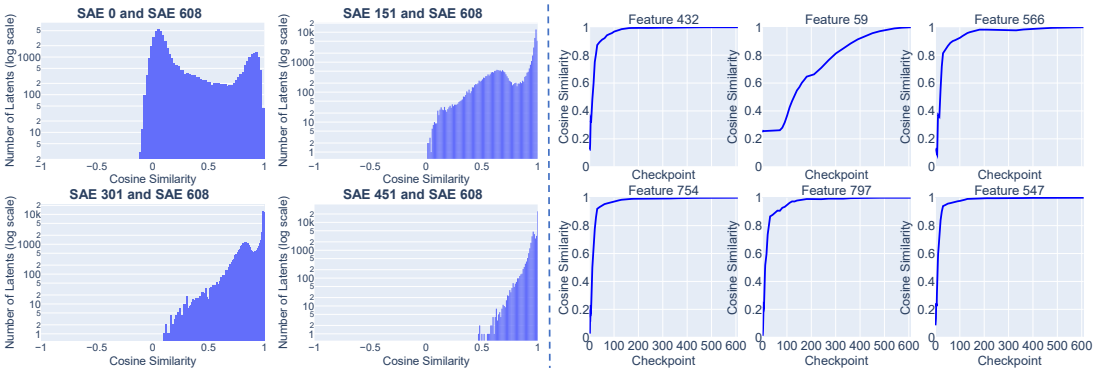

Figure 23. **Cosine Similarity for stanford-gpt2-small-a.**

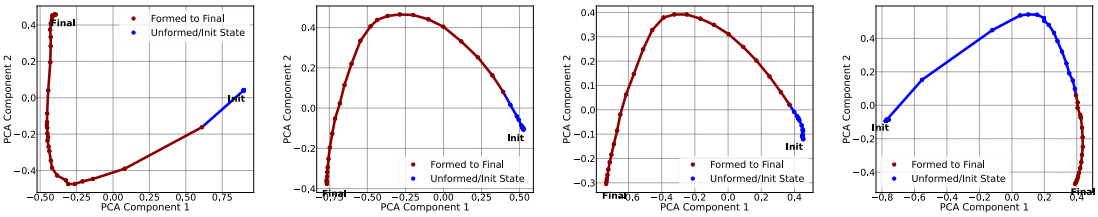

Figure 24. **Feature Trajectories for stanford-gpt2-small-a.**

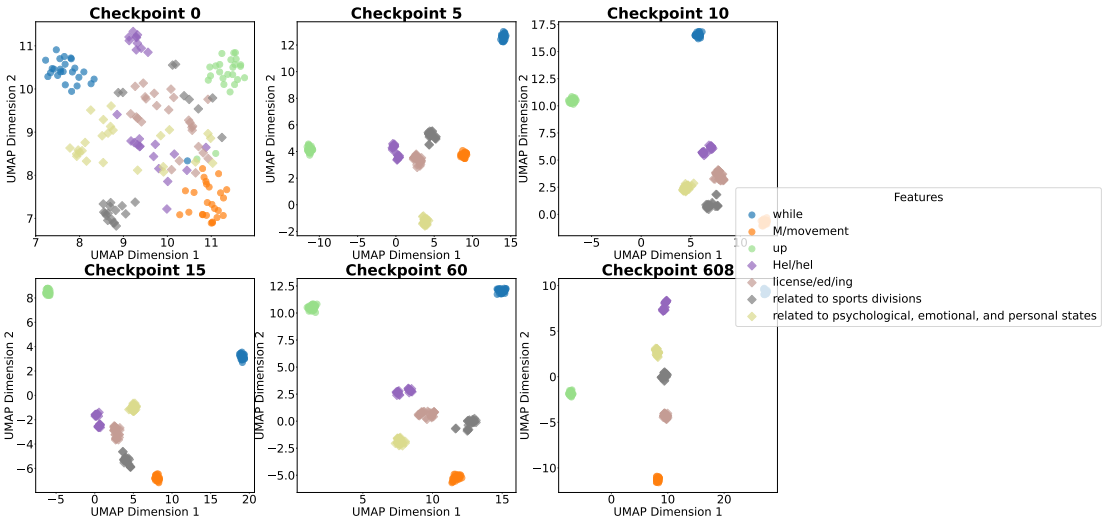

Figure 25. **UMAP for stanford-gpt2-small-a.**

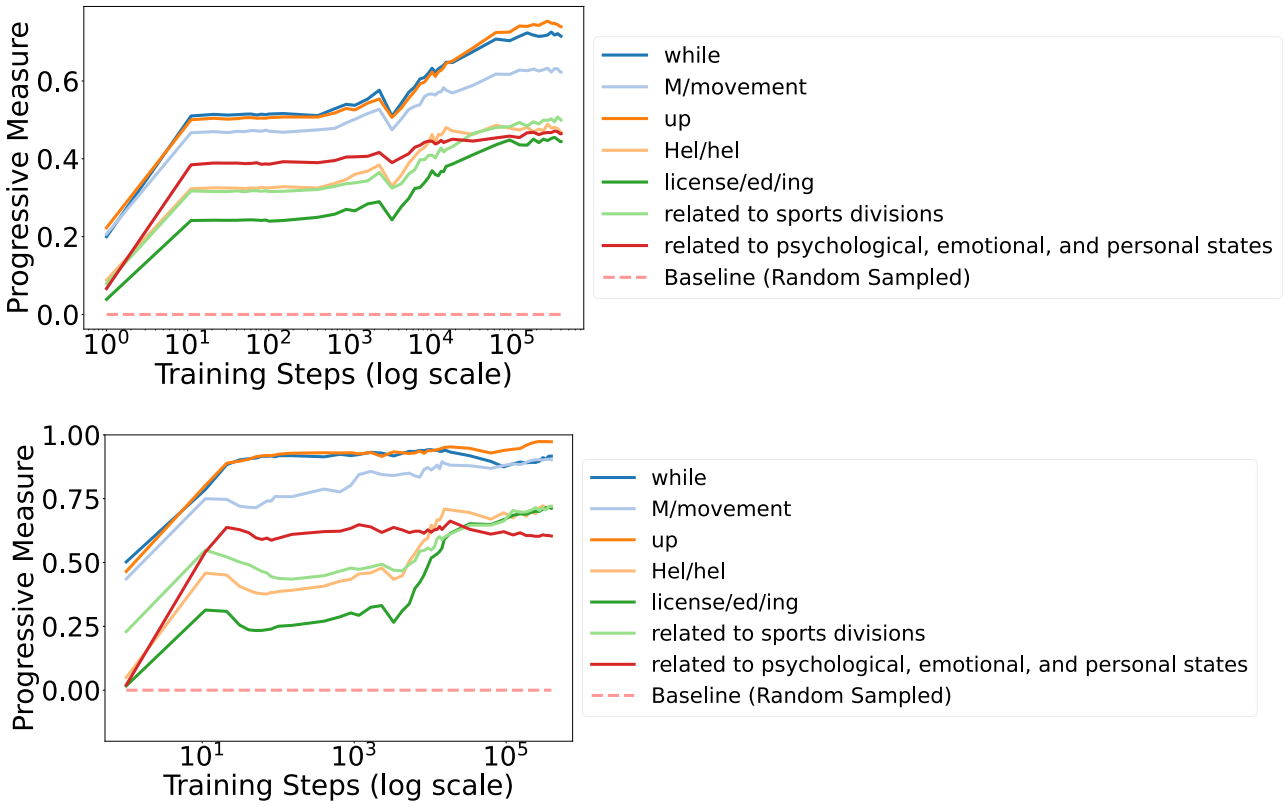

Figure 26. **Progress Measure for stanford-gpt2-medium-a.** The top represents the activation space, while the bottom represents the feature space.

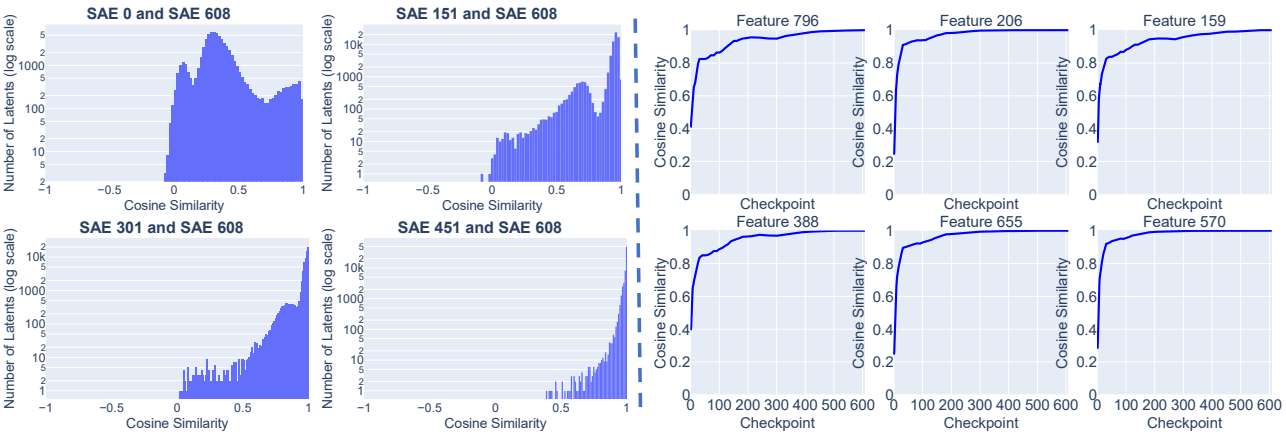

Figure 27. **Cosine Similarity for stanford-gpt2-medium-a.**

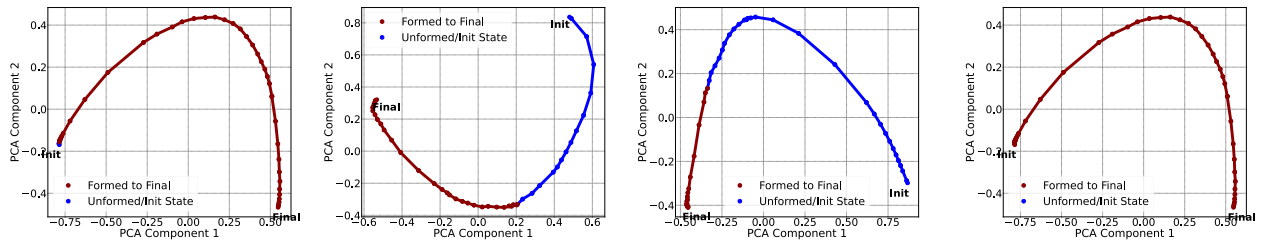

Figure 28. **Feature Trajectories for stanford-gpt2-medium-a.**

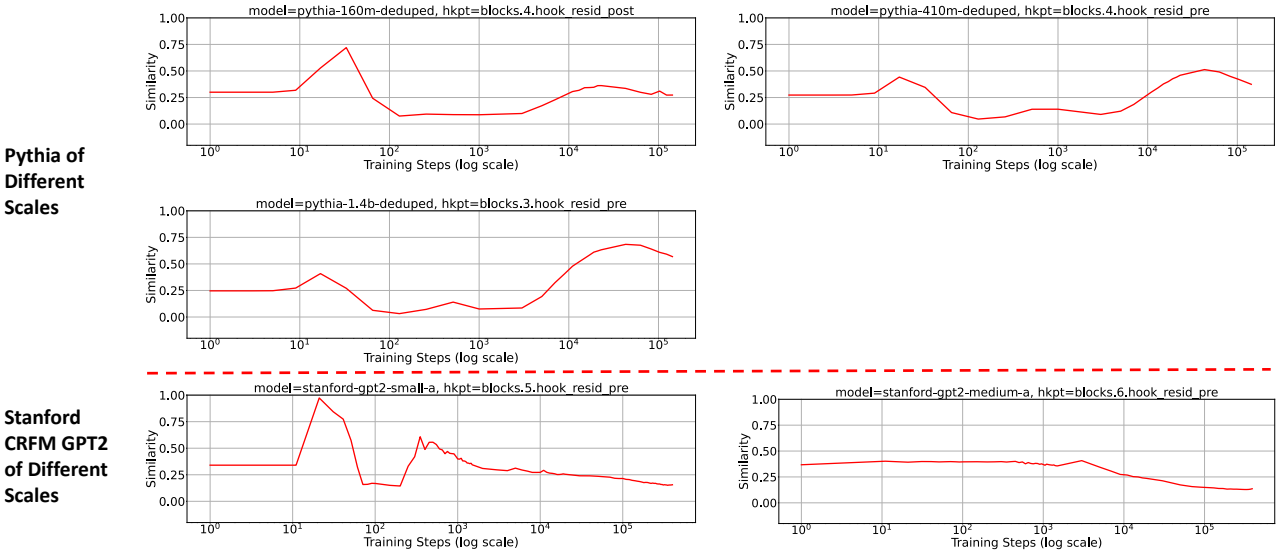

Figure 29. **Feature Collapse**

I. Possible Feature Collapse

We observe a phenomenon we refer to as **feature collapse** in the early checkpoints of certain models (e.g., GPT-2-small-a, where it is most pronounced).

Feature collapse, in this context, refers to a state where all activations or features converge to near-1 cosine similarity. This phenomenon manifests as a glitch in the our measure (Fig. 4), which we attribute to a sudden burst in $\overline{\text{Sim}}_{\mathcal{A}_{\text{random}}}$ (Figure 29). Specifically, when $\overline{\text{Sim}}_{\mathcal{A}_{\text{random}}}$ approaches 1, such that $1 - \overline{\text{Sim}}_{\mathcal{A}_{\text{random}}} < \epsilon$, and given that $\overline{\text{Sim}}_{\mathcal{A}_i^t} \leq 1$, the measure $M_i(t) = \overline{\text{Sim}}_{\mathcal{A}_i^t} - \overline{\text{Sim}}_{\mathcal{A}_{\text{random}}}$ becomes suppressed to near-zero values ($< \epsilon$), leading to the glitch.

I.1. Model-Specific Phenomenon

This collapse is model-specific and may be linked to optimization settings, particularly during early training. Notably, we find that this behavior parallels observations in (Liu et al., 2022), where the cosine similarity of activations (referred to as "features" in their work but analogous to "activations" in our context) increases significantly in early training before decreasing. The observed increase in cosine similarity in our context induces the collapse, as it artificially reduces the ability of any metric to distinguish features.

I.2. Impact on SAE-Track

When feature collapse is severe(where $\overline{\text{Sim}}_{\mathcal{A}_{\text{random}}}$ rapidly approaches 1), it causes disruptions in the tracking process. Specifically, SAE-Track may exhibit phase shifts near the collapse point, reflecting distinct deviations. This is because feature collapse compromises SAE's ability to preserve feature properties, making tracking behavior more unstable and inconsistent.

However, severe feature collapse does not always occur in LLMs (only one of the LLMs we tested exhibited severe feature collapse). When it does occur, it typically happens at a very early point in training, where we still retain a long and compact tracking range for the remaining training process. So SAE-Track remains capable of preserving the majority of feature information and provides complete and accurate tracking beyond this point. By focusing on checkpoints after the collapse, we ensure that the feature trajectories remain stable and interpretable in the subsequent analysis.

J. Research Impact and Future Directions

Here, we discuss the broader impact of our work beyond the main paper.

J.1. Broader Impact on the Field of Mechanistic Interpretability

SAE for Interpretability, Research on Training Dynamics, and Beyond:

- **Understanding what the model learns during training.** Previous work (Bricken et al., 2023) has demonstrated that SAE-based interpretation not only reveals information about the data but also provides insights into the model itself, as shown by comparisons between features in randomized and trained Transformers. Our work fills the gap by systematically analyzing how features transition from those in a **randomized Transformer** to a fully **trained Transformer**, offering a mechanistic view of this process.
- **Unveiling the geometric and semantic structure of feature evolution.** While SAEs trained at different checkpoints retain sparsity and can reconstruct activations in a similar manner, the extracted features—except for some token-level ones—are noisy in an untrained LLM. This is because datapoints with similar semantic meanings do not yet form distinct geometric localities in the activation space. From our **geometric perspective** (feature regions), feature formation becomes more intuitive, which is difficult to observe directly from conventional metrics such as reconstruction loss and sparsity. This corrects potential misconceptions that SAE structures remain unchanged during training.
- **A novel SAE training framework with potential applications to fine-tuning.** The SAE-Track framework not only enables efficient tracking of features across training checkpoints but also provides a structured way to investigate changes during fine-tuning. Applying this method to fine-tuned models could reveal how learned features are modified or repurposed in response to new objectives.

J.2. Future Research Directions

Potential directions are listed below:

- **Real-Time Intervention.** SAE-Track enables the synchronous training of SAEs alongside LLMs at a low computational cost, facilitating real-time supervision using SAE. Given that feature formation is a gradual and progressive process, this framework allows for the early detection and mitigation of unsafe or undesired features before they solidify. Furthermore, SAE-Track can be extended to the fine-tuning stage, providing similar capabilities for monitoring and guiding feature adaptation during model refinement. Previous studies have explored interventions or alignment using SAEs (Templeton et al., 2024; Farrell et al., 2024; Chalnev et al., 2024; Yin et al., 2024). Our approach offers a promising direction for enhancing model safety and alignment by enabling proactive feature monitoring throughout training.
- **Feature Drift and Theoretical Insights into Model Optimization.** Our study reveals that feature drift persists even after features gain semantic meaning, suggesting a deeper connection between feature evolution and the model's optimization process. Investigating this relationship could provide insights into both model training dynamics and optimization theory. Future work may explore the mechanism of how optimization methods affect drift.
- **Finer-Grained Concept Spectrum.** As discussed in Appendix C, A finer-grained and quantitative analysis of this could provide deeper insights into LLM's features.